Avasarala and Bose
Functional Composite Materials (2023) 4:5
https://doi.org/10.1186/s42252-023-00042-2

Functional Composite Materials

REVIEW

Open Access

2D nanochannels and huge specific surface area offer unique ways for water remediation and adsorption: assessing the strengths of hexagonal boron nitride in separation technology

Sankeerthana Avasarala[1] and Suryasarathi Bose[1*]

Abstract

This review highlights the advantages of incorporating hexagonal Boron Nitride (BN) into the current membrane-based architectures for water remediation over other well-explored 2D nanomaterials such as graphene, graphene oxide, molybdenum sulphide, MXenes. BN has an interlayer spacing of $3.3A^0$ which is similar to that of graphene, but smaller than that of the other 2D nanomaterials. BN is bioinert, and stable under harsh chemical and thermal conditions. When combined with thin film composite and mixed matrix membrane architectures, BN can help achieve high permeance, dye rejection, and desalination. Laminar membranes assembled by BN nanosheets do not swell uncontrollably in aqueous environments unlike graphene oxide. BN nanomaterials have a large specific surface area which implies more adsorption sites, and are inherently hydrophobic in nature, which means the adsorbent in its powder form can be easily separated from contaminated water. BN adsorbents can be regenerated by treating with chemicals or heating to high temperatures to remove the adsorbate, without damaging the BN, due to its thermal and chemical inertness. BN nanomaterials have the potential to circumvent the current shortcomings of membranes and adsorbents, while greatly enhancing the performance of membranes and adsorbents for water remediation.

Keywords Hexagonal boron nitride, 2D nanomaterials, Membrane, Adsorbent, Dye and antibiotics removal, Desalination, Antifouling, Oil–water separation

*Correspondence:
Suryasarathi Bose
sbose@iisc.ac.in
Full list of author information is available at the end of the article

Graphical Abstract

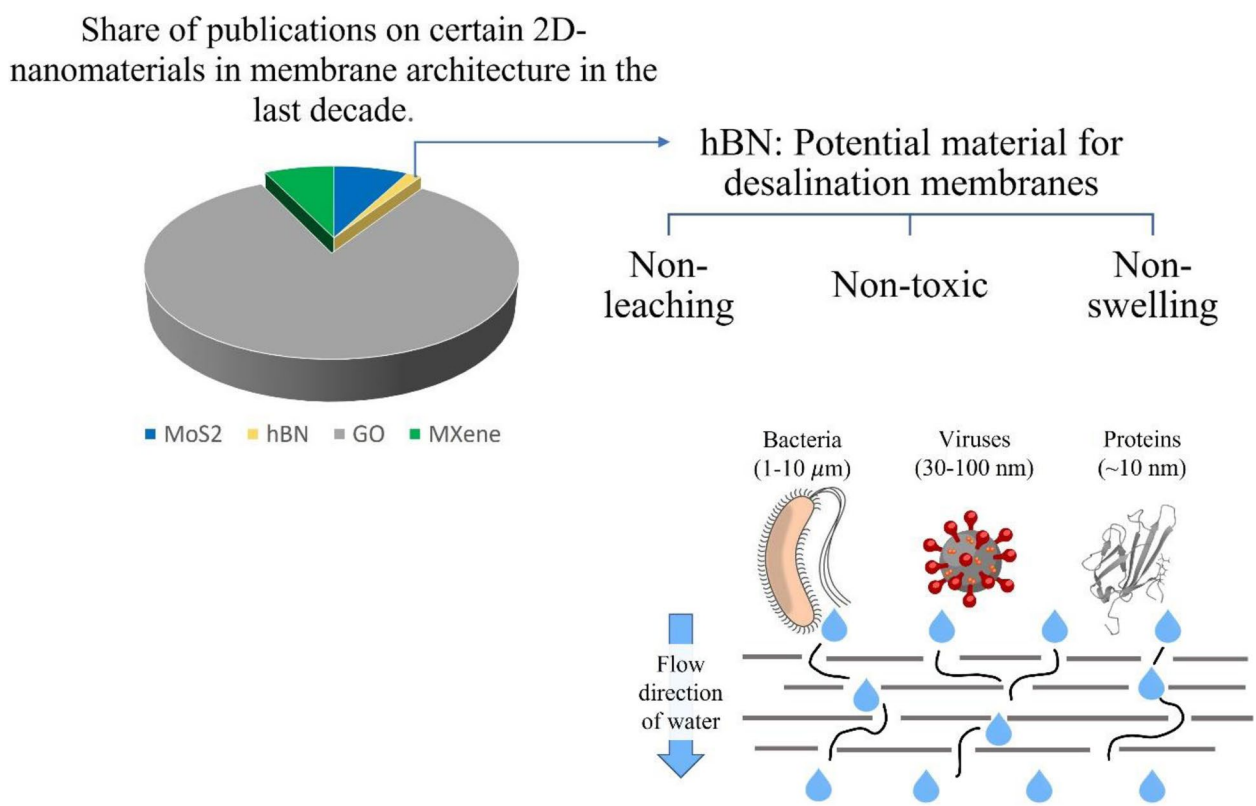

Introduction

The availability of clean water is one of the most critical issues globally, now more so than ever. With the ever-expanding population of the world and the diminishing sources of fresh groundwater, it is proving increasingly challenging to meet the clean water needs of the modern world [1]. There is an urgent need for innovation and technology to face the global water challenge. Amongst the most prevalent ways of water remediation, membrane-based filtration methods hold the reins compared to their counterparts due to their high separation efficiency, low thermal energy input, and high-quality output. Polymer-based membranes are the most prevalent in all the filtration regimes – microfiltration (MF), ultrafiltration (UF), nanofiltration (NF), reverse osmosis (RO), as these are easy to process on an industrial scale, and their properties can be tuned to suit the end requirement. In the RO and NF regimes, polyamide-based thin-film composite (PA-TFC) membranes currently rule the market as these are easy to process, offer control over the thickness of the active polyamide layer, and most importantly, have high rejection rates of salts and other micropollutants. However, the current state-of-the-art polyamide desalination membranes are only twice as porous as they were 20 years ago, with the same selectivity.

These membranes are still chlorine intolerant, which makes disinfection cumbersome and increases membrane fouling and thus reduces its filtration capacity [1]. Water transport occurs through the solution-diffusion mechanism- a relatively slow process. NF and RO membranes suffer from low flux, severe fouling, and high energy input. In addition, RO systems require post filtration steps like remineralization. These are some of the reasons that led to the Government of India to completely ban the domestic usage of RO, unless required.

Although the research on PA-TFC membranes continues to move ahead at full throttle, these shortcomings have prompted researchers to search for alternative materials. Considering that there is a need for a breakthrough membrane technology with high water-to-solute selectivity if the needs of future generations are to be met, 2D nanomaterials seem to be the ideal candidates for this purpose. The isolation of graphene in 2004 at

the University of Manchester sparked a revolution in the study and application of 2D nanomaterials in various disparate fields. Membrane technology is no exception. The last decade has seen an explosion of research on water filtration membranes based on these nanomaterials. 2D nanomaterials possess nanometer level thickness, leading to higher flux, large surface area, which results in numerous transport pathways and greater area for solute-surface interaction, vast array of tunable properties that can be tailored to meet the filtration needs, and nanometer-thick transport channels and pores. These nanomaterials can be incorporated into the polymer matrix to obtain mixed matrix membranes, they can be free-standing porous 2D membranes, or can be deposited as an active layer atop a support membrane [2, 3]. The numerous ways in which nanomaterials can be used to enhance the performance of existing membranes and to fabricate completely new high-performance membrane systems is what propels the thriving research. These materials have been the focus of extensive research in the last few years. This review aims to bring the reader up to date by highlighting the work done on BN-based water purification membranes specifically and Graphene, MXenes and MoS_2 based membranes generally. Unless mentioned otherwise, BN here implies hexagonal boron nitride.

BN is made up of boron and nitrogen arranged alternatingly forming a hexagonal pattern in each monolayer. The monolayers follow an ABAB stacking pattern, due to the van der Waals forces between the monolayers as well the partial positive and negative charges on boron and nitrogen respectively. In the following sections, a few studies on graphene and graphene oxide, dichalcogenides, MXenes are discussed followed by a thorough survey of membrane applications and the role as an adsorbent of hexagonal boron nitride, which is the material of focus of this article. This review for the most part includes only the experimental studies involving these nanomaterials. As this review focuses on BN, the reader is referred to other general works on GO, MXenes, Dichalcogenides in their respective sections.

2D nanomaterials for water purification (membranes)

While the transport of solutes, water and other solvents occurs through solution-diffusion in RO membranes, and through convection in the UF and MF membranes and a combination of convection and diffusion in NF membranes, the transport in 2D NMs occurs through molecular sieving through nanochannels and nanopores, and electrostatic interactions. 2D nanomaterials possess a host of desirable properties. A few have even been found to be anti-bacterial. The sections on each of the nanomaterials will illustrate, through studies, the properties that make these materials superior in water filtration applications.

Graphene and graphene oxide

Studies on membranes based on graphene and its derivatives have burgeoned in the last few years because of their potential to enhance, if not replace, the performance of current water purification membranes. This can be attributed to the thinness, large surface area, vast array of tunable properties, pliability in terms of functionalization, mechanical strength, antimicrobial activity, and low density of graphene and its derivatives [3, 4]. In pristine graphene, carbon atoms that are sp^2 hybridized are arranged in a hexagonal pattern in a single layer, about 0.34 nm thick [5]. The atomic-level thickness of the layers results in very thin laminar membranes with high flux, even thinner than the typical 100 nm polyamide active layer [6]. Additionally, graphene shows better resistance to chlorine compared to polyamide. In its pristine form, graphene is impermeable to water. This can be circumvented by introducing nanopores into the sheets, as demonstrated in a modelling study by Suk and Aluru. Water flux observed was greater than that of CNT when the pore diameter was larger than 0.8 nm [7]. Although other studies have corroborated the high water permeability values along with salt rejection via sieving through the nanopores [8], fabrication of large, leak-free single layer graphene with controlled pore size and pore size distribution on an industrial scale remains an issue. On the other hand, graphene oxide (GO) is a derivative of graphene made by chemical oxidation and ultrasonic exfoliation of graphite and is easy to fabricate on a large scale. Depending on the degree of oxidation, GO consists of graphene sheets with hydroxyl, epoxide, carboxyl, and carbonyl groups in varying fractions, which increases the interlayer spacing to over 0.6 nm. These sheets can be easily stacked to form laminar structures held together by hydrogen bonding [5, 9]. Multilayer GO membranes are highly permeable to water because of the porous microstructure which includes the space between the edges of adjacent sheets, wide channels at wrinkles, and nanopores in the sheets. The latter contributes negligibly to multilayer structures. The selectivity of these membranes depends on the interlayer spacing, electrostatic interactions between the negatively charged sheets and ions, and ion adsorption effects like cation-π and metal coordination to the sheets [10–12]. The major shortcoming of GO membranes, due to the presence of hydrophilic groups, is their uncontrollable swelling and instability on hydration, which largely increases the interlayer spacing and affects sieving ability. This can be controlled to an extent by reducing or chemically cross-linking the GO sheets, or stitching them to a polyamide layer [13, 14]. Other

shortcomings of GO multilayered membranes include low mechanical stability and low desalination capacity [15, 16]. Extensive work has been done on membranes based on graphene and its derivatives in the past decade. For detailed reviews of the same, the reader is directed to references [4, 5, 10, 11, 15, 16].

Transition metal dichalcogenides (TMD)

TMDs are a class of materials with the formula MX_2 where M is a transition metal element from groups IV, V or VI and X is S, Se or Te, i.e. chalcogens. These materials form laminar structures of the form X—M—X, with the chalcogen atoms in two hexagonal planes separated by a plane of metal atoms. Adjacent layers are held together by weak van der Waals forces [17]. One TMD that has been extensively studied for applications in electronics, and more recently in membranes is MoS_2. With the S atoms above and below the Mo plane, these layers are smooth due to the absence of functional groups unlike in GO, which can result in unimpeded water flow due to low hydraulic resistance. The absence of extruding hydrophilic functional groups also means that van der Waals forces dominate instead of weak electrostatic forces and lead to stability in aqueous media. As each sheet is made up of 3 atomic layers, MoS_2 is robust under pressure unlike GO where the nanochannels tend to undergo elastic deformation under pressure. Due to an abundance of S atoms, MoS_2 has highly negative zeta potential which imparts good dispersibility. There are numerous ways to obtain the 2D nanosheets of these materials, which have been discussed in detailed in refs [17, 18].

Laminar structured MoS_2 membranes can be fabricated for molecular separation. Sun et al. were the first to report such a membrane through vacuum filtration of chemically exfoliated MoS_2 sheets on to a polycarbonate porous support. The resulting membrane showed 3–5 times higher permeance than GO, with similar rejection performance for 3 nm sized molecules for the same membrane thickness. The thin sheets partially overlap leading to many empty spaces which serve as the nanochannels. These nanochannels were found to be unperturbed even under high pressure, unlike in GO where the nanochannels suffer elastic deformation [19, 20].

Another study which corroborated these observations was conducted by Wang et al. An MoS_2 membrane was fabricated by vacuum filtration onto a PES porous support post organolithium intercalation and forced hydration. The interlayer spacing was 1.2 nm (free spacing 0.9 nm) post hydration, which remained unchanged even after soaking in water for 3 days. In comparison, the interlayer spacing of GO of similar thickness increased from 0.8 nm to 5.2 nm following excessive swelling. On drying, the interlayer spacing was 0.62 nm (free spacing 0.3 nm), same as that of bulk MoS_2 due to the restacking of the sheets, which makes it almost impermeable to water [19]. Ries et al. reported stable MoS_2 free-standing membranes through covalent functionalization with acetamide, methyl, and ethyl-2-ol groups using organohalides. The membranes exhibited superior desalination and organic molecule rejection compared to GO based laminate membranes. Through molecular dynamics simulation of water flow in the nanochannels, the team observed that the water velocity is enhanced in methyl functionalized membrane compared to the pristine one. This was attributed to the pinning of water molecules right underneath the S atoms due to the interactions between highly polarized O–H and Mo-S bonds, which slowed the local velocity in the pristine MoS_2 membrane.

On the other hand, the methyl groups substituted some of the pinning points and enhanced the overall velocity [21]. MoS_2 sheets with nanopores also hold the potential to work as desalination membranes. In a simulation study by Heiranian et al., a 0.2–0.6 nm^2 area pore in an MoS_2 monolayer could reject 88% ions and predict a pure water flux 2–3 times that of other nanoporous 2D materials [18].

Many other studies have been carried out with MoS_2 nanosheets- one group recently designed an MoS_2 nanosheets-silk nanofibril hybrid membrane inspired by nacre shell structure [22], another group developed a MoS_2/GO hybrid membrane for dye and salt removal [23]. Numerous studies have also reported the ability of MoS_2 nanosheets to adsorb heavy metals from water [24–26].

MXenes

MXenes (pronounced Maxenes) are a class of 2D transition metal carbides, nitrides, and carbonitrides that were discovered in 2011 by researchers at Drexel University [27]. MXenes have a general formula of $M_{n+1}X_nT_x$ ($n = 1–3$), where M, as an early transition metal (such as W, Mo, Cr, Ta, V, Nb, Hf, Zr, Ti, Y, or Sc), X is carbon and/or nitrogen, and T denotes the surface termination groups such as fluorine (–F), oxygen (–O), chlorine (–Cl) and hydroxyl (–OH), and x represents the number of surface functionalities. The surface functionalities are a result of the etching and exfoliation of the MAX phase generally in aqueous media [27, 28]. In the precursor MAX phase, the A (Al or Si) layer is sandwiched within octahedral $M_{n+1}X_n$, where the strong M-X bond has a mixed covalent/metallic/ionic character whereas the weak M-A bond is metallic in nature. Exploiting the weak nature of the M-A bond, the A layers can be selectively etched out keeping the structure intact going from the 3D MAX phases to a 2D morphology. What makes MXenes stand out is the numerous possible

combinations of transition metals. The goal is to find the stable ones, currently an area of great interest for researchers. Titanium based MXenes have been explored the most, such as $Ti_3C_2T_x$, $Ti_2C_1T_x$ with nitrides, carbides and carbonitrides. $Ti_3C_2T_x$ can be obtained, for example, by etching the MAX phase Ti_3AlC_2 with hydrogen fluoride. The unique structure of MXenes imparts various characteristics such as high surface area, hydrophilicity, biocompatibility, high electrical conductivity, ease of functionalization. These properties make them ideal for use in energy storage applications, electronics, sensors, catalysis, environmental remediation, water purification [28, 29]. Like other 2D nanomaterials, MXenes can be used as a filler in polymeric composites, or directly as a membrane on top of a support layer. MXenes have also been shown to be antibacterial, good adsorbents, and have ultrafast water transport and ionic sieving abilities.

Ren et al. created a $Ti_3C_2T_x$ membrane though vacuum assisted filtration of its colloidal solution containing 1 nm thick sheets, on to a PVDF (polyvinylidene fluoride) support. The membrane showed greater selectivity for metal cations than GO. The ion selectivity was based on charge as well as the hydrated size of the ions, indicating the potential use of MXenes for water softening. MXenes are negatively charged. MXenes reject cations with hydration shell bigger than the interlayer spacing. MXenes can selectively aid ion permeation for cations which have a hydrated diameter smaller than the interlayer spacing such as Na^+ and Mg^{2+}. The Na^+ ions intercalate into the MXene gallery easily and get attached to the sheets on either sides, eventually leading the sheets covered with Na^+ to repel each other and slightly expands the gallery, resulting in higher permeation. On the other hand, for divalent and trivalent cations, the mechanism is slightly different. When these multivalent ions penetrate into the MXene gallery, there is a slight expansion in the gallery first, but as more multivalent ion enter the galley the electrostatic attraction between the cations and the negatively charged MXene sheets overtakes, tightening the gallery and slowing down the permeation of multivalent cations. Higher permeance was observed compared to GO membrane of the same thickness, which could be because of the narrow, uniform 2D nanochannels of 6.4 A^0, due to the high aspect ratio of the sheets [30].

Biofouling is a major problem in membrane filtration, which is why membrane materials that exhibit antibacterial properties are desired. In a study by Rasool et al., antibacterial action of Ti_3C_2Tx colloidal solution was observed against Escherichia coli (E. coli) and Bacillus subtilis (B. subtilis). The MXenes damaged bacterial cell membranes, releasing its cytoplasmic material. They were also found to have higher antibacterial activity than GO, for the same colloidal concentration [31]. Although it has been experimentally demonstrated that MXenes show antibacterial activity, the exact mechanisms for the same are still under active research. Rasool et al. observed that the bactericidal activity of MXenes is concentration dependent, and damages the bacterial cell membrane through direct penetration. This study does not however conclude on the contribution of reactive oxygen species, if any, on the bacteriocidal activity of MXenes [31]. Further, another work by Rsool et al. extended the above mentioned work to study the effect of MXene membrane aging on its bactericidal properties by keeping the membrane in ambient atmosphere for 1 month. Surprisingly, they observed enhanced bactericidal activity after aging the membrane, compared to the freshly made membranes. This was attributed to the formation of anatase TiO_2 and defective 2D carbon on aging of the MXene membrane, which along with the MXenes aid in physical penetration of the bacterial cell membrane. Additionally, the group mentions that reactive oxygen species could have been generated from TiO_2 which could have aided in the enhancement as well, but the effect of the latter has not been quantitatively demonstrated [32]. A simulation study by One-Sun Lee et al. investigated the possible mechanism for antibacterial activity of MXenes using molecular dynamics. The study observed that the MXenes get adsorbed on the bacterial cell membrane and cause a phase transition leading to a phase boundary defect, which further causes the intracellular material to leak, damaging the bacteria [33]. For a comprehensive study on the proposed mechanisms for the antibacterial activity of MXenes, the reader is directed to the recent review article on the same by Salimiyan Rizi [34].

MXenes have also been fabricated into membranes for oil–water separation, dye removal and desalination [35]. Another interesting application was illustrated by Zha et al., where a flexible, solar-driven water purification membrane was fabricated using MXenes and cellulose fibres [36]. Insanullah has discussed more applications of MXenes in water remediation in reference [27, 28]. MXenes are a relatively new entrant into the 2D nanomaterials market and there exist significant issues that need be addressed to translate the lab research to an industrial scale. Some of these include the use of toxic chemicals for etching out the Al from Ti_3AlC_2, limited knowledge of the potential toxicity and biocompatibility of MXenes and based membranes, and most importantly, their short shelf life as they degrade quickly in the open [28, 37]. Clearly, this promising nanomaterial's potential is yet to be fully explored once its shortcomings are addressed.

Structure, properties, and synthesis of hexagonal boron nitride

Boron nitride has a structure similar to graphene, in its 2D form, so it is also called 'white graphene'. The boron and nitrogen atoms are covalently bonded with a partial positive and partial negative charge on boron and nitrogen respectively and arranged alternatingly, in a hexagonal manner, in each (mono)layer. The nanosheets consist of a few hexagonal boron nitride layers with an interlayer spacing of 0.33 nm, held together by weak van der Waals forces. Due to the electronegativity difference, the electron pairs of the B-N σ bond are more confined towards nitrogen than boron. In the case of graphene, there is complete delocalization and equal sharing of the π electrons between the C atoms, whereas the lone pair of the p_z orbital of nitrogen is only partially delocalized with that of boron, resulting in partial positive and negative charges on boron and nitrogen atoms respectively. This results in a stacking pattern where the B of each layer is between the N of the layers above and below it [38]. Typically, exfoliated BN is in the form of flakes consisting of 2–5 monolayers, but can vary according to the synthesis, exfoliation and further functionalization routes. The lateral dimensions of the flakes are 100–300 nm, while the lateral size of bulk BN can be 2-10 μm. BN has a density of about 2.2 g/cc, a melting point of around 2800 ℃ [39–41]. BN has high mechanical strength, making it ideal as a reinforcing agent in certain polymers [42]. Pristine BN is inherently hydrophobic in nature.

BN possesses high chemical inertness and oxidative resistance due to its structure. 2D laminar membranes made by stacking BN flakes have numerous nanochannels with large surface area because of the flakes' high length to thickness (aspect) ratio. The higher aspect ratio makes the nanochannels tortuous for contaminants. It also simultaneously increases the likelihood that the contaminants come in contact with the surface of the hBN flakes, to prevent or enhance their permeation through specific interactions, depending on the end requirement. The surface of BN is overall negatively charged, which has been attributed to the presence of adsorbed hydroxyl groups, according to Pendse et al. At a higher pH, an abundance of hydroxyl groups results in higher negative charge [43]. These unique set of properties renders BN ideal for a host of applications ranging from water remediation and osmotic energy conversion to electronics and drug delivery.

BN is a very good adsorbent for heavy metals such as Cr(III), Cd(II), dyes like rhodamine B (RB) and organic molecules like tetracycline and a wide range of oils. The excellent adsorption capacity has been attributed to the polarity of the B-N bond (which makes it particularly suitable for metal ion chemisorption), high specific surface area, and surface defects. A major advantage of BN as an adsorbent for organics is its high thermal stability, making the regeneration relatively easy by simply heating to high temperatures to burn the adsorbed organics, making it reusable. Additionally due to the inertness of hBN to harsh chemicals, substances adsorbed onto hBN can be removed by treated them with these harsh chemicals, while BN remains intact [44–47]. Studies have shown that BN is biocompatible and more than carbon nanomaterials and can be used as implant materials. One recent study demonstrated that BN, as a therapeutic agent, accelerated wound healing. The potential for BN in medicinal applications is attributed to its excellent chemical stability and mechanical strength, absorption in the UV region, and low toxicity [38, 48].

The structure and properties of 2D nanomaterials are determined by techniques used to synthesize them, and the processing steps thereafter. For membrane applications, a high yield of BN with large lateral dimensions is desired to stack the sheets to make galleries which create tortuous pathways for contaminants, as mentioned earlier. There are many methods for fabricating BN, including chemical vapor deposition, epitaxy, mechanical and chemical exfoliation. Each technique has its advantages and disadvantages. Chemical vapor deposition and epitaxy involve high temperatures and gaseous atmospheres which produce BN with inherent defects over which there is little control, but the number of layers and the dimensions over a large scale can be controlled in these methods. On the other hand, mechanical and chemical exfoliation, though relatively cost-effective and good for large scale production, have low yield and produce flakes with a broad size distribution and offer no control over the number of layers. Other techniques include pulsed laser deposition, physical vapor deposition and pyrolysis of boron and nitrogen containing compounds [39]. A detailed review of these techniques for synthesis of BN can be found in reference [39]. To tailor the properties of BN to the application, it can be functionalized with different functional groups and polymers. The numerous ways demonstrated for functionalizing BN nanostructures have been detailed in the review references [38, 39]. Going forward, the sections on the applications of BN in water purification membranes and adsorbents will give a better insight into the effect of structure, properties, and the synthesis routes of BN on the performance of membranes and adsorbents in the various works mentioned.

Applications of BN in water purification

BN based membranes

As mentioned earlier, the thin sheet-like structure, high surface area, small interlayer spacing, excellent thermal and chemical stability, and oxidative resistance, negative

surface charge, amongst other qualities make BN an ideal candidate for applications in water purification membranes. Modelling and simulations studies on water and ion transport through nanopores in the BN monolayers and through the interlayer spacing, have demonstrated enhanced transport performance. Simulation studies by Gorbanfekr et al. show that the water transport is faster between the layers of BN due to low friction (Fig. 1) [49]. Another simulation study by Tocci et al. discusses the transport of water at nanoscale, in contact with BN sheets [50]. Yet another simulation study by Liu et al. proposes that the nanoslit patterns in BN monolayers can affect the water transport and the ion rejection performance of BN nanosheet membranes [51]. Jafarzadeh et al. in their simulation study of the ion rejection performance of nanoporous BN nanosheets, demonstrate that functionalizing the nanopore with fluorine and hydroxyl groups can improve its filtration performance [52]. Since this review focuses on the experimental studies on filtration performance of BN based membrane architectures, only a few simulation studies are mentioned on the same. From the above studies, it can be concluded that the absence of functional groups lead to a friction free transport of water through the nanochannels made by stacking hBN sheets into a gallery, assuming non porous sheets. If the hBN sheets have pores, it can further aid in the transport of water by reducing the path traveled by the water molecules through the hBN gallery, while rejecting ions with hydration shell greater than the size of the nanopores. Further modification of the nanopores with functional groups such as hydroxyl or fluorine has been proposed to aid in the ion rejection through the nanopores through specific interactions between these and the ions.

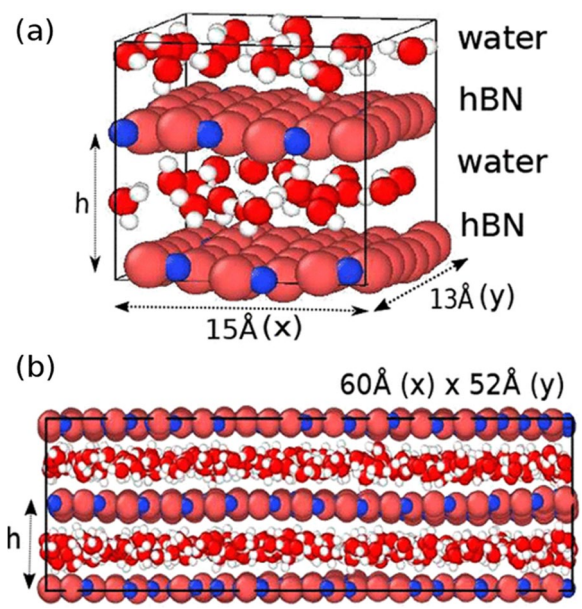

Fig. 1 System of nanoconfined water molecules (red and white balls) between BN membranes (blue and pink balls) with nanometric interlayer distance *h* for typical **a** Density Functional Theory and **b** Molecular Dynamics supercells. Reprinted with permission from reference [49]. Copyright 2020 American Chemical Society

With a combination of various synthesis, exfoliation and functionalization strategies, this decade has seen numerous works on the use of BN as a membrane, a foam, a reinforcing agent, an adsorbent, a surface modifier, and more. Following are experimental studies conducted on applications of BN in water filtration membranes, followed by a section on its applications as an adsorbent. Each of these works will help in understanding the properties of BN that are specifically applicable for water purification, through various architectures.

Lei et al. synthesized porous BN nanosheets of high porosity and specific surface area to demonstrate its sorption properties for oils, organic solvents, and dyes (Fig. 2). The porous nanosheets showed fast absorption kinetics and high mass uptake (up to 33 times their own weight for ethylene glycol) compared to other common adsorbents of oils and organic solvents. This has been attributed to adsorption, capillary effects, and intercalation because of the hydrophobic nature and polarity of the B-N bond. The porous nanosheets outperformed other absorbents for dye sorption as well. The absorbent was easily collected as the nanosheets floated on water and were regenerated by heating in air or solvent extraction, which were possible because of the excellent thermal and chemical stability of BN. This regeneration capacity over multiple absorption cycles makes BN stand out [53]. Lei et al. also developed aerogels and flexible, free-standing membranes from amine functionalized BN. The latter was prepared through vacuum filtration. This is notable because the group used a high yield and the relatively simple and scalable exfoliation and functionalization process of ball-milling BN with urea. This is a mechano-chemical exfoliation in which shear forces exfoliate the BN sheets and simultaneously decompose urea, prompting the NH_2 groups to attach to the edges and defects of the BN layers [40].

Like other 2D nanomaterials, BN can be infused into a polymer matrix to enhance its properties. Liu et al. developed a composite porous BN/PVDF membrane through non-solvent induced phase inversion, by adding BN to the PVDF dope solution. The permeability of both water and organic solvents obtained was thrice that of neat PVDF due to the highly cross-linked networks between porous nanosheets and PVDF. A 99.99% separation was obtained for oil/water emulsions, pharmaceuticals were filtered up to 14L/g and organic dyes up to 9.3L/g. The

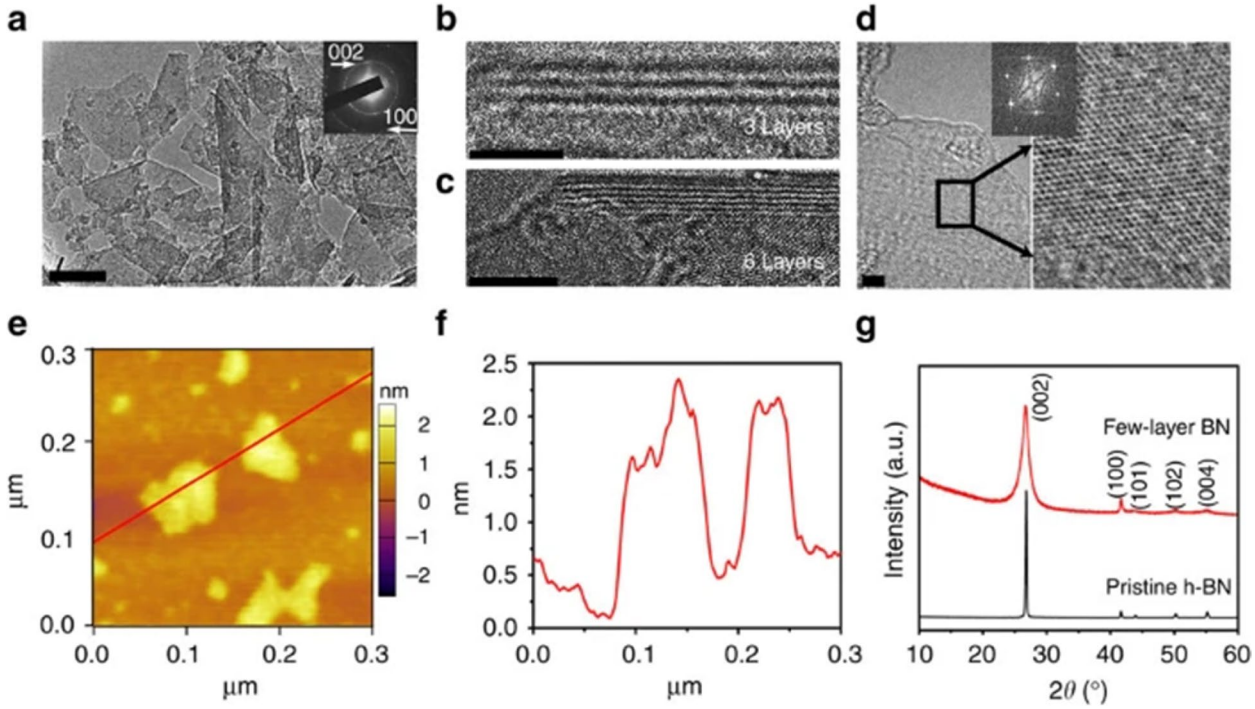

Fig. 2 Exfoliated few-layer BN. **a** TEM image of few-layer BN, with the selected-area electron diffraction pattern (inset) indicating a layered BN structure. Scale bar, 50 nm. **b**, **c** HRTEM images of the edge folding of two few-layer BN sheets with three and six BN layers, respectively. Scale bars, 2 nm (**b**) and 5 nm (**c**). **d** HRTEM and the fast Fourier transform images of a few-layer BN sheet. Scale bar, 2 nm. **e**, **f** Atomic force microscopy image and corresponding line-scan profile of few-layer BN. **g** XRD patterns of few-layer BN and pristine h-BN. (Reprinted from ref. [40] under Creative Commons License)

filtration performance was attributed to the polarity of the B-N bond, high porosity, and specific surface area of the nanosheets. The membranes could be recycled as well [54].

Marichy et al. developed a well-crystallized, self-standing BN membrane using a combined atomic layer deposition (ALD) and polymer derived ceramic (PDC) route with control of through porosity in terms of size and shape. The cylindrical pores obtained ranged from a few tens to hundreds of nanometers. These membranes, even though brittle, could be inserted into a suitable porous support and indicate potential use in osmotic energy conversion and water filtration [55].

A thin film nanocomposite nanofiltration membrane was fabricated by Abdikheibari et al., where 0.004wt% amine functionalized BN (modified through ball-milling with urea) was added to the aqueous solution of piperazine and interfacial polymerization was carried out with trimesoyl chloride on a porous polyethersulfone support. The nanosheets, embedded in the polyamide layer, enhanced the hydrophilicity and the free volume available for water flow, thus increasing the flux as well as the fouling resistance. A 13.4% improvement in the flux and a 5.2% increase in natural organic matter (NOM) rejection was observed. 0.97 of the initial flux was maintained when a humic acid solution was filtered [42]. Another architecture developed by the same group involved deposition of amine functionalized BN(0.003wt%) on top of the polyamide layer of piperazine and trimesoyl chloride on polyethersulfone porous support. This resulted in a smooth, hydrophilic surface with a negative charge, which led to a 59% increase in flux and 50% increase in resistance to fouling by NOM. Sodium alginate and bovine serum albumin rejection was above 92% [56].

The earlier works incorporated BN into the matrix of the polymer membranes by adding them to the dope solutions. Gonzalez-Ortiz et al., on the other hand, developed a BN/polyvinylalcohol (PVA) microfiltration membrane through pickering emulsion templating. Here, BN was used as an emulsion stabilizer and to enhance the mechanical and antifouling properties due to its high hardness, corrosion, and oxidation resistance. PVA was added to an aqueous dispersion of exfoliated BN, followed by ethyl benzoate, which resulted in a homogeneous emulsion post sonication. The BN sheets would adsorb at the liquid–liquid interface, form a rigid shell around the droplets, and prevent coalescence. This was cast onto a glass substrate, cured, and immersed in a bath

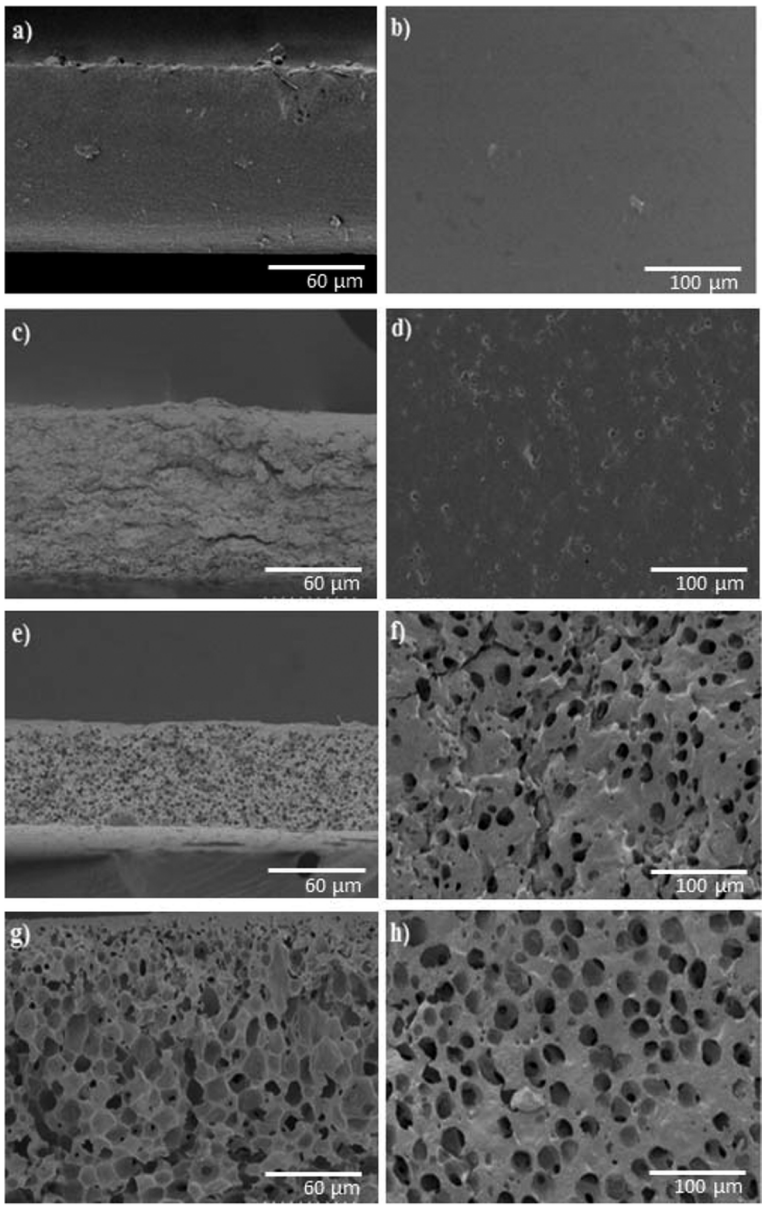

Fig. 3 SEM images of the h-BNNS/PVA porous membranes depending on the curing time before crosslinking: **a** cross-section of single PVA, **b** surface of single PVA, **c** cross-section of BNP-24 h, **d** surface of BNP-24 h, **e** cross-section of BNP-3 h, **f** surface of BNP-3 h, **g** cross-section of BNP-1 h and **h** surface of BNP-1 h. Reproduced from Ref. [57] with permission from the Royal Society of Chemistry

containing ethanol, HCl and glutaraldehyde for cross-linking, as PVA is water soluble otherwise. The curing time was found to greatly affect the pore size and porosity of the resulting membrane (Fig. 3). For a certain curing time and corresponding pore size, the membrane was found to reject 76% of polystyrene latex nanoparticles of size 0.1 µm and 99.7% of the particles of size 1.2 µm. The membrane showed higher permeance and rejection capabilities than the PVA based membranes fabricated through other conventional methods such as thermally induced phase separation or Electrospinning. More importantly, this method was green—free from harmful reactants and waste generation [57].

Low et al. fabricated a polyethersulfone/BN mixed matrix nanofiltration membrane through non-solvent induced phase separation. An aqueous dispersion of BN was sonicated with sodium dodecyl sulfate and added to the dope solution. The resulting membrane was more hydrophobic, more negatively charged, due to the inherent hydrophobicity of BN and its negative charge. While

the neat PES membrane only recovered 80% water flux on fouling, the PES/BN membrane recovered the flux completely. The permeance increased but the rejection, as tested with the dye Rose Bengal, decreased by a small amount owing to BN acting as a plasticizer [58].

The addition of BN to the membrane matrix generally makes the surface denser, rougher, more hydrophobic and increases the permeance. The rugged surface is a result of the nodular structures on the membrane surface due to solid–liquid de-mixing, in which BN acts as nuclei for crystallization and partly because of aggregation of BN nanosheets. To demonstrate this, Zahirifar et al. incorporated BN into PVDF to develop a membrane for air-gap membrane distillation via non-solvent induced phase separation and BN was added to the casting solution. It also enhanced the thermal stability of the membrane along with an 18% increase in the tensile strength. These improvements could be credited to the excellent thermal and mechanical strength of BN itself [59].

Although relatively easy to fabricate, mixed matrix membranes may not always fully exploit the properties of 2D nanomaterials such as their high aspect ratio and specific surface area, nanoscale interlayer distance, etc. On the other hand, laminar membranes formed by stacking sheets of 2D nanomaterials offer desirable molecular separation based on electrostatic interactions and sieving, through nanopores and nanochannels. Following are studies on the same, giving insight into the mechanisms of transport in such membranes.

Chen et al. developed a multipurpose thin functionalized BN (FBN) membrane through vacuum filtration onto a nylon support to separate mixtures. BN powder was functionalized by ball-milling with urea. The flakes were 1.2 nm high and 100–300 nm in lateral dimensions. Each flake consisted of 4–5 monolayers. The thickness of the FBN layer could be varied by changing the volume of their aqueous dispersion. Permeation tests of toluene, p-xylene, pyrene, and rhodamine B were conducted in ethanol and water. RhB was fully blocked, while permeation of acetone in water and toluene in water was 5.8 and 2.2 times that through GO, respectively. Permeation was on par with that of MXene laminar membranes. The short and abundant transport pathways in the FBN membrane rendered such high flux possible, along with the excellent thermal and chemical stability of BN itself, which kept the structure stable. Membranes were stable even after solvation for 24 h in acetone, ethanol, hexane, toluene, and water as well as in extreme pH environments [60].

Another work by Chen et al. involved pressure driven filtration studies of the FBN membrane on a nylon support in organic solvents. Dye rejection tests were performed with Methylene Blue, Acid Fuschin, Evans Blue and Congo Red in Methanol. A 0.4 μm thick FBN layer showed 99% rejection for gold nanoparticles (5 nm) and > 99% rejection for congo red. The water flux was 1.5 and 16 times greater than of MXenes (0.1–0.4 μm thick) and reduced graphene oxide (2 μm thick) membranes respectively, reported in literature. The performance was ascribed to the hydrophilicity, the stability of the flakes and the spaces between them, and the structure of the nanochannels, which depended on the lateral size of the flakes, the height of the nanochannels, and the gap size between the edges of the flakes [61].

Ultrafast permeation of ions was observed through an FBN membrane on a cellulose ester support by Chen et al. The 200 nm thick FBN membrane essentially acted as a mesh with a pore size of 8.6 A^0, as it completely rejected ions with hydrated radii greater than 4.3 A^0. The membrane exhibited ultrafast permeation with a permeation rate of nearly 9 mol m-2 h-1 for sodium ions for smaller hydrated ions, nearly 25 times faster than the theoretical diffusion rate. Small ions such as Na^+, K^+, Mg^{2+}, Ca^{2+} and Zn^{2+} permeated quickly while larger ions and molecules such as Mn^{2+}, sucrose and glycerol were much slower to permeate or did not permeate at all (Fig. 4). Their observations indicated that permeation rates were influenced by the mass, size, charge, and hydration radii of the ions and the concentration of feed solution and surface charge of the membrane [41].

The above experiments involved functionalizing BN with amine groups, which reduces the negative surface charge of BN, as Pendse et al. argue. They created a membrane where exfoliated BN, via bath and probe sonication, was vacuum filtered onto an AAO (Anodized Aluminium Oxide) porous support to get a 10 μm thick layer. By not functionalizing the BN, the group chose to exploit the highly negative surface charge of BN while reducing the processing steps. To demonstrate that the filtration property depends on the size of the sieving channels as well as the surface charge, filtration tests were performed with dyes and salts across a wide range of charges and molecular sizes. The estimated size of the nanochannels was 1.2–5 nm and zeta potential of BN was calculated to be −60 to −70 mV between a pH of 8 and 10 [43]. The negative surface charge was estimated to be caused by the adsorption of hydroxyl ions on the surface of the BN, which would only increase at a higher pH. The membrane outperformed other membranes based on functionalized BN, MXenes, dichalcogenides, graphene and derivatives in terms of small anion rejection and water permeability [43].

Hybrid membranes fabricated using two different nanomaterials can offer a synergistic effect and circumvent the limitations that might show up when using each material separately. For instance, Lin et al. developed an

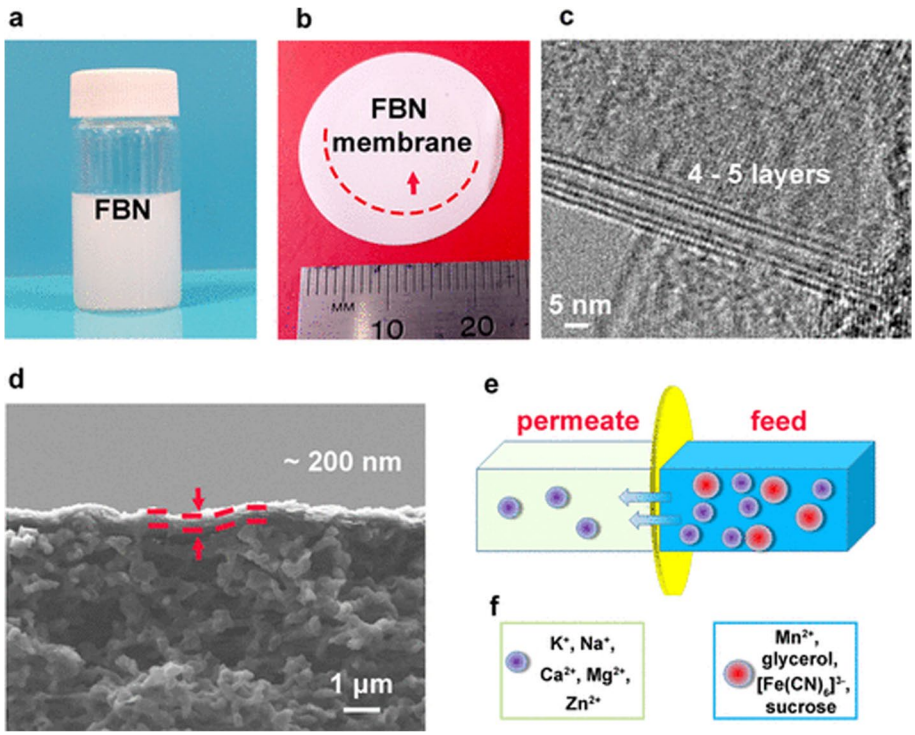

Fig. 4 **a** Photograph of FBN water dispersion. **b** Photograph of the FBN membrane. The FBN membrane is highlighted with a red dash line to distinguish it from the support membrane. **c** TEM image of the edge of an FBN flake. **d** Cross-sectional SEM image of the FBN membrane with a thickness of 200 nm supported on a filter membrane. **e** Schematic diagram of the permeation of different ions through FBN membranes. **f** Tested species, the left box shows the ions that can pass through the FBN membrane, whereas the right box illustrates the hydrated ions and molecules that are blocked by the FBN membrane. Reprinted (adapted) with permission from reference [41]. Copyright 2019 American Chemical Society

amine functionalized BN and GO hybrid membrane on a polydopamine coated porous PES support. The major problem of instability and excessive swelling of GO in aqueous media was solved by alternately depositing GO and BN resulting a tightly packed laminar stacking. The covalent bonding between the edges of the two nanomaterials stabilized and prevented the GO from swelling. This also created sufficient nanochannels for water permeance and dye rejection. The resulting membrane was found to be stable across solutions of different pH. A rejection rate > 99.5% was observed for methylene blue across hybrid membranes of varying GO and BN concentration. The water flux varied from 1–4.5 LMH at 300psi, across different compositions [62].

Osmotic energy generation from seawater is a promising alternative source of energy with low environmental impact. Also called salinity gradient energy or blue energy, it make use of the salinity gradient between seawater and river water which causes an osmotic pressure difference. The membranes used to generate power from salinity gradients must have high mechanical strength, thermal and chemical stability- to withstand the lifecycle of osmotic energy generation plants- combined with high salt rejection values for pressure retarded osmosis. Stable nanochannels formed by the interlayer gallery of membranes made from 2D nanomaterials present an opportunity to exploit this blue energy through reverse electrodialysis and pressure retarded osmosis. Chen et al. created a cartilage inspired BN-aramide nanofiber composite membrane via layer-by-layer assembly to meet these requirements, making a hybrid of 2D nanomaterials and 1D nanofibres. BN was chosen because of its superior thermal and chemical stability, and stability in a variety of solvents and extreme pH environments in addition to its ultrafast water and ion transport properties, which are the major requirements for membranes used for osmotic energy generation. BN was ball-milled with glucose for hydroxyl groups. Aramid nanofibres were added to impart mechanical robustness to prevent microcracks under pressure and to create additional transport pathways. A glass substrate treated with poly(diallyldimethylammonium) chloride polycation (PDDA) was immersed in aramid nanofiber and BN suspensions alternately for a certain number of steps (n) to create a multilayered nanocomposite membrane which they termed as ABN_n. ABN_{30} was flexible and only 1 μm thick. The layers are held together strongly by dense hydrogen bonds between the nanosheets and the fibers.

This resulted in a tensile strength of 370 MPa, which was much greater than that of membranes made only from BN or aramide nanofibers. They demonstrated that ABN_{30} membranes in tandem could power a digital timer [63].

Yazda et al. fabricated a BN/SiN hybrid membrane with nanopores in the sub 10 nm range through a technique called tip-controlled local breakdown, using an atomic force microscope, for osmotic power generation. With a pore-to-pore spacing of 500 nm, they concluded that the mechanical stability provided by SiN and the high surface charge density of BN resulted in a power density of 15 Wm^{-2} when using KCl as the electrolyte. Their technique allowed for precise control over the size and the distribution of pores in the BN layer [64].

Keshebo et al. fabricated a BN lamellar membrane by vacuum filtration of its aqueous dispersion containing tannic acid onto a Nylon support membrane. Tannic acid acted as a green exfoliating agent by specifically interacting with the BN layers and thereby reducing the BN interlayer attraction. It also helps the BN nanosheets adhere to the Nylon support membrane. The resulting membrane showed > 99% rejection of congo red, and a high antifouling tendency against humic acid even after 7 cyles [65].

It can be concluded from the above works that exploiting the properties of BN relevant to the applications- such as its hydrophobic nature, tunable sheet size as well as surface area according to the synthesis routes, its capacity to withstand high temperatures, harsh chemical environments, and its mechanical strength- the overall properties of the membranes could be significantly enhanced. Although the research on applications of BN in membrane-based technology is relatively in early stages, it suggests optimistic results in effective nanofiltration and desalination membranes for the future.

BN based adsorbents

The adsorption performance of any adsorbent is evaluated in terms of the following factors. Ideally, the adsorbents should demonstrate high separation selectivity and high adsorption capacity, quick uptake, easy regeneration, and multiple cycling ability. Unless mentioned otherwise, 1 cycle includes an adsorption as well as a desorption cycle. The absorbent should also exhibit high gravimetric capacity, should be easy to deploy and recover after the adsorption process. Since boron and nitrogen are light elements, boron nitride absorbents would have large gravimetric capacity. BN has high chemical and thermal stability. This means that BN adsorbents can be regenerated by simply heating at high temperatures to remove the adsorbed organics, without destroying the structural integrity of the adsorbent, or can be washed with various solvents and chemicals to remove the adsorbed contaminants. The adsorbed substances can also be removed using solvent extraction or broken down using harsh chemicals, without damaging BN since it exhibits very high chemical inertness. Since nanomaterials have a large specific surface area, adsorbents made from BN nanomaterials would be ideal as they combine the properties of nanoscale materials with properties of BN [47, 53].

Das et al. fabricated a non-functionalized BN membrane through vacuum filtration of a suspension of boron nitride nanosheets in NMP and IPA onto a PVDF support membrane. After performing filtration tests with BPA (a neutral solute), MO and DR-80(anionic dyes), for a certain optimum thickness of the lamellar membrane, they concluded that the retention was driven by the adsorption of these pollutants to the BN sheets. They found the effects of size exclusion or Donnan exclusion to be negligible in this case. The membrane showed high stability even in an acidic environment, and recovered 90% of its dye absorption capacity after 4 cycles of rejection indicating the reusability of the membrane [66].

Lei et al. synthesized boron nitride nanosheets using boron trioxide and guanidine hydrochloride as the boron and nitrogen precursors respectively. Since a high temperature of 1100 ℃ was used for the synthesis, nitrogen, hydrogen chloride and ammonia gases are released from the decomposition of guanidine hydrochloride, which created pores of a few tens of nanometers in the boron nitride nanosheets over a micron in their lateral dimensions. Here, the porosity is due to the pores in the nanosheets as well as the spaces between the sheets themselves. After the oils and organic solvents were adsorbed from water, the group studied the XRD patterns of the BN adsorbent before and after the adsorption process. According to the XRD patterns, the interlayer spacing in the porous boron nitride nanosheets increases slightly as the oils and organic solvent molecules intercalate into interlayer spacing due to its porosity and inherent hydrophobicity. The percentage change in the interlayer spacing would depend on the adsorbate and the adsorbent-adsorbate affinity as well. Comparatively, the interlayer spacing of commercial bulk BN remains unchanged even after saturation with oil and organic solvent. This ability of porous BN to slightly swell and accommodate adsorbent molecules while still maintaining its structural stability has been correlated to its greater adsorption capacity compared to the commercial bulk BN [53]. Liang, G. et al. came up with a creative route to synthesize a nanonet from BN nanofibers, with NH_4BF_4 and NaN_3 as precursors while using CS_2 as a catalyst through a solvothermal process at 260 °C (Fig. 5). The nanonet, which was made up of 8 nm thin BN nanofibers, was able to adsorb methylene blue from

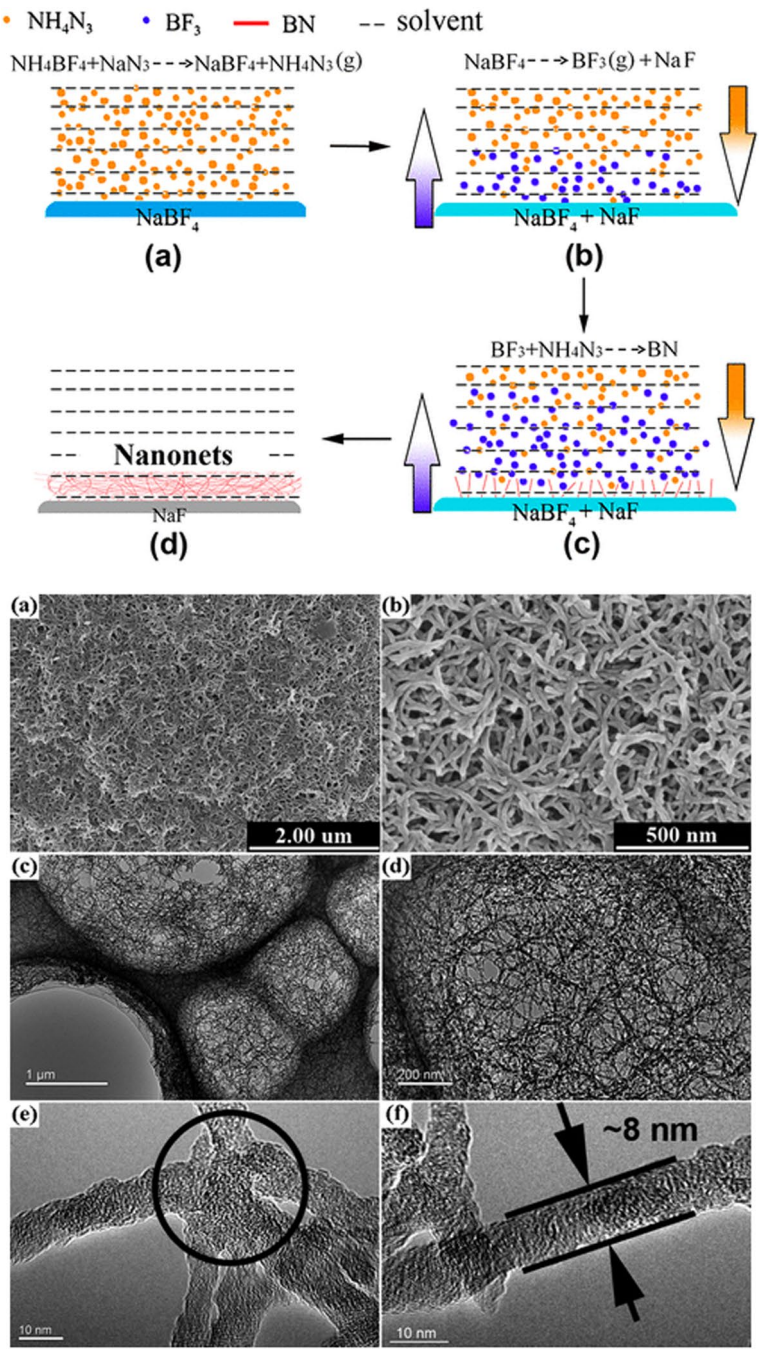

Fig. 5 Schematic Illustration of the Formation Process of BN Ultrathin Fibrous Nanonets. BN ultrathin fibrous nanonets prepared by one-step solvothermal process with CS2 as the catalysts. **a**, **b** Typical SEM images and **c**, **d** the corresponding TEM images of BN nanonet with different magnification ratios; **e**, **f** HRTEM images of a typical fibrous knot (circled) and a BN nanofiber with diameter of ~8 nm. Reprinted with permission from reference [67]. Copyright 2013 American Chemical Society

water, and sieve Au nanoparticles with respect to their size when used as a membrane [67].

Lian Gang et al. synthesized BN nanospheres with outer diameters of 50–300 nm using a template free route, for hydrogen storage as well as organic pollutant removal from water. The nanospheres showed preferential adsorption for basic yellow 1, an aromatic dye molecule even in the presence of $CuSO_4$, a heavy metal ion. This has been attributed to the specific non-covalent interaction between the aromatic rings and hBN,

similar to the π-π interactions observed in graphene and its derivatives [68]. Liu et al. also synthesized boron nitride spheres high absorption capacity for a range of heavy metals and organic dyes [69]. Theoretical studies have reported that BN shows only weak interactions with hydrogen, but some experimental works have shown otherwise, so the use of BN in hydrogen storage needs to be delved into further [70, 71]. Along with H_2 adsorption and storage, hBN has also been touted as a prospective material for CO_2 capture [72–74].

Li, J., Xiao, X., Xu, X. et al. synthesized "activated BN" by adding a surfactant to the precursors during the synthesis of BN. The activated BN had a ribbon like structure, which were porous and rough. The BN obtained here had a d-spacing of 0.35 nm, which is slightly greater than that of hBN (0.33 nm). The activated BN performed better than porous BN and activated carbon as well, in the case of adsorption of Co^{2+}, Ni^{2+}, Ce^{3+} and Pb^{2+}, tetracycline, methyl orange and congo red. According to the group, the surfactant added during synthesis helped increase the surface area and pore volume and the adsorption ability, but the exact mechanism is yet to be elucidated [44]. Apart from the presence of functional groups, the number of defect sites and the degree of crystallinity also influences the performance of BN. Li, Jie, et al. synthesized BN fibres which was more crystalline in nature which they claim imparts stability to the adsorbent during the absorption–desorption process, compared to the activated BN using a surfactant in their previous work (discussed in the previous paragraph). They further activated these fibres with a mixture of sulphuric acid and nitric acid treatment, which created defects and functional groups at the edges of BN while maintaining its crystallinity mostly intact (as corroborated by their XRD plots and TEM micrographs) and increasing the absorption capacity [75]. Rod like porous hBN has been synthesized by Song et al. for antibiotic adsorption, specifically tetracycline-based compounds here. The microporosity and mesoporous nature is concluded from the adsorption isotherms and the adsorption–desorption hysteresis curves [76]. hBN has been synthesized in various forms for adsorption of different antibiotics, and bisphenol A as well, which is a toxic substance prominent in the food packaging industries [77, 78].

In the above-mentioned work, the different forms of BN were synthesized as a powder, and used as a powder for the adsorption experiments, which tends to agglomerate during adsorption and desorption, which can limit its performance. Hence, Jie Li et al. synthesized activated BN embedded with NaOH groups, in a 3D form to increase the surface area of interaction of the pollutants with the adsorbent, while maintaining structural stability. NaOH-3D BN was prepared to adsorb HCOH and simultaneously act as a support for its catalytic degradation. Its porous structure has been attributed to the interfacial spaces between the nanoflakes. HCHO removal on NaOH-3D BN were much higher than those of the NaOH-embedded commercially activated carbon and the NaOH-embedded activated BN. NaON-3D BN was regenerated just by using an electric hair dryer and retained its HCHO adsorption capacity of 90.5% for 15 cycles. The embedded NaOH converts the toxic HCHO to relatively less toxic methoxy and formate salts [79].

Yanming Xue et al., fabricated a boron nitride porous monolith (BNPM) for dye and heavy metal removal as well as oil–water separation. The group first prepared a boric acid-dissolved formaldehyde-dicyandiamide resin as the precursor in the form of a rod-like monolith, which was porous because of the gases formed during the resin solidification reaction, which bubbled through to escape and resulted in a porous precursor monolith. This precursor solid was then pyrolyzed above 1000 ℃ in ammonia

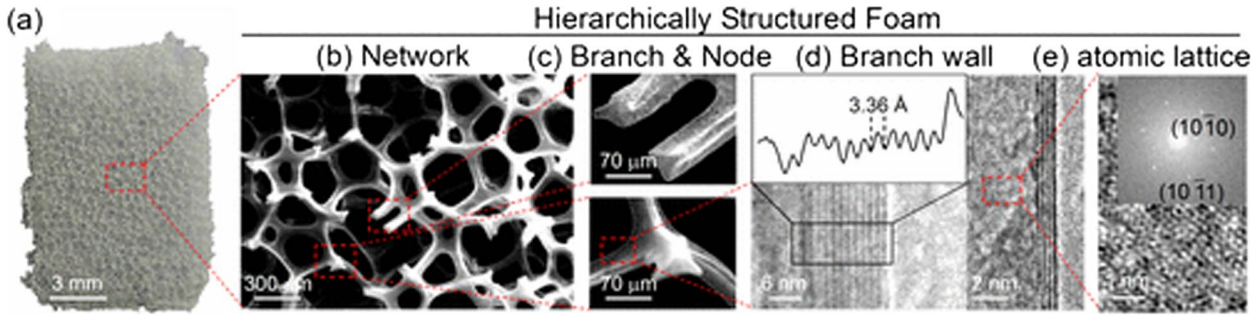

Fig. 6 Hierarchical structures of the free-standing BN foam. **a** Photograph of a free-standing BN foam. **b** SEM image of a BN foam network. **c** Magnified SEM images of two branches and a node. **d** High-resolution TEM images of BN sheets near their folded edges, where the number of dark lines for the edges indicates the thickness of 12 and 4 layers, respectively. The interlayer spacing obtained from the edges is ~0.34 nm. **e** High-magnification TEM image and its fast Fourier transform (inset), indicating the typical hexagonal lattice of the BN sheet. Reprinted with permission from reference [80]. Copyright 2013 American Chemical Society

atmosphere under ammonia flow to obtain a BN porous monolith. The BNPM showed excellent oil adsorption capacity and could be easily regenerated by burning the adsorbed organic substances in air. BNPM also showed high adsorption for rhodamine B dye and Copper (II) ions from water due the hydroxy and amine groups residing on the walls of micropores and holes of BNPM. The dye was removed from BNPM using ethanol. The group explained how the hierarchical structure enhances the adsorption of oil, dye, or organic molecules onto boron nitride. Although the boron nitride is in its turbostatic form, the concept of a hierarchical structure for adsorption can be applied for applied across different materials, and boron nitride in its hexagonal form as well. The macropores allow unrestricted pathways for pollutants to diffuse though. The large number of micropores then provide abundant surfaces for the pollutants to adsorb onto. Since boron nitride is inherently hydrophobic, the micropores allow oils to flow into and fill up the pores through capillary action. Next, the surface interaction plays the major role in adsorption of dye molecules and heavy metal ions. The pore walls, pore network, nodes and defects present in the structure of boron nitride, as well the functional groups (if any) influence the dye and heavy metal adsorption [45]. The role of hierarchical structure of porous architectures of adsorbents is discussed in the work by Jun Yin et al. on the boron nitride foam synthesized using CVD, discussed in the following paragraph.

Jun Yin et al. fabricated BN foams with a network of hollow tubes via CVD using borazane as the precursor and a Nickel foam as the template. The foam could recover completely even after compression up to 70%. As shown in the SEM and TEM micrographs of the foam in Fig. 6, it is made ofhierarchical structures- foam-like macrostructure, hundreds of micrometers porous network, hollow-tube-like branches and nodes at tens of micrometers, branch wall consisting of a few BN layers, and atomic lattice of hexagonal BN (Fig. 6) [80].

2D nanomaterials have large specific surface area but using the adsorbent in a powder form has certain drawbacks as well. Due to the aggregation tendency of these powders during absorption process, their uptake could be hindered. To circumvent this, three-dimensional (3D) architectures can be made with 2D nanomaterials. These 3D architectures are lightweight, have very low densities, and can create hierarchical porous structures while retaining the inherent features of 2D nanomaterials. These 3D forms are also relatively easier to handle compared to the powder form of BN, that is, to deploy and recover because of their structural stability [81, 82]. Zhao, H. et al. synthesized a 3D BN foam which they called "3D WG", where WG stands for white graphene, as hexagonal boron nitride is isostructural to graphene but is white in color. Using thiourea and aminothiourea as vesicants which were added to ammoniaborane as the precursor. The CS_2, NH_3 and NCNS gases released aided in the foaming. they obtained a low-density 3D WG foam with pore sizes ranging from a few nanometers to microns. The foam could absorb a range of organic solvents up to 70–190 times its weight and had higher organic dye adsorption in comparison to other forms of BN such as hollow spheres [68] fibrous nanonets [67], nanocarpets [83] and porous nanosheets [53]. Liu, Z., Fang, Y., Jia, H.

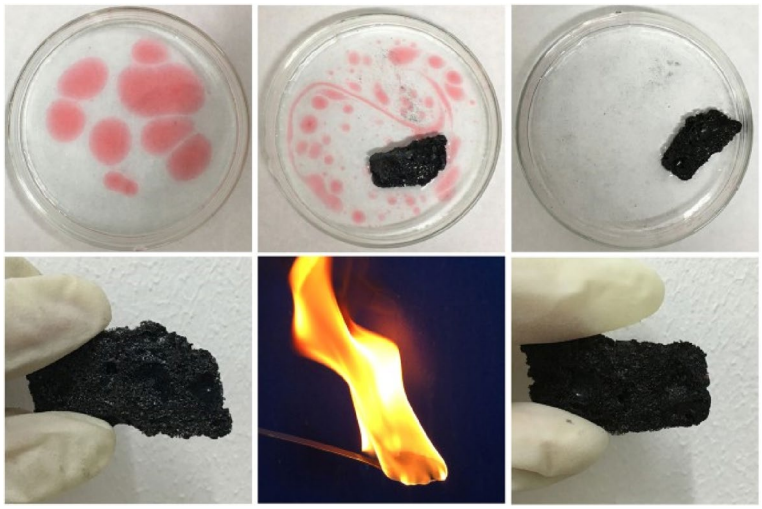

Fig. 7 **a**–**c** The process of adsorbing gasoline by 3D C-BN; **d** Original appearance of the 3D C-BN; **e** Burning the sample after absorbing gasoline; **f** The appearance of 3D C-BN after six times recycling. Reproduced from reference [84] under the Creative Commons license. https://creativecommons.org/licenses/by/4.0/

Table 1 Recent works involving applications of BN in separation applications

S. No	Reference	Architecture	Application	Performance
1	Ref. 53 Lei et al. (Porous boron nitride nanosheets for effective water cleaning) [53]	Exfoliated BN nanosheets	Absorption of dyes, organic solvents, and oils	Ethanol, Toluene, Pump oil, Used Engine oil, Ethylene Glycol absorption ranging between 2000–3300%
2	Ref. 40 Lei et al. (Boron nitride colloidal solutions, ultralight aerogels and freestanding membranes through one-step exfoliation and functionalization) [40]	Aerogel, free-standing membranes of BN nanosheets	Proof of concept	-
3	Ref. 54 Liu et al. (Multifunctional Polymer/Porous Boron Nitride Nanosheet Membranes for Superior Trapping Emulsified Oils and Organic Molecules) [54]	BN nanosheets incorporated into PVDF-Mixed matrix membrane	Oil–water separation, Dye and pharmaceutical rejection	Carbamazapine, ciprofloxacin, chlortetracycline: 100% removal upto a critical concentration of BN in the membranes
4	Ref. 55 Marichy et al. (Fabrication of BN membranes containing high density of cylindrical pores using an elegant approach) [55]	Free-standing BN membrane through atomic layer deposition	Proof of concept	-
5	Ref. 42 Abdikheibari et al. (Thin film nanocomposite nanofiltration membranes from amine functionalized-boron nitride/polypiperazine amide with enhanced flux and fouling resistance) [42]	BN nanosheets embedded in the Polyamide layer of a thin film composite membrane	Fouling resistance	97% of the initial flux retained during filtration with 120 ppm humic acid solution
6	Ref. 56 Abdikheibari et al. (Novel thin film nanocomposite membranes decorated with few-layered boron nitride nanosheets for simultaneously enhanced water flux and organic fouling resistance) [56]	BN nanosheets deposited on top of the Polyamide layer of a thin film composite membrane	Fouling resistance	Sodium alginate and bovine serum albumin separation maintained over 92% over 3 cycles, 59% increase in fouling resistance on addition of BN
7	Ref. 60 Chen et al. (Functionalized boron nitride membranes with multipurpose and super-stable semi-permeability in solvents) [60]	BN nanosheets deposited onto a porous nylon support	Solvent separation	Permeation rates of 1.5 – 2.5 mmol m^{-2} h^{-1} of paraxylene over pyrene (0.5 mol m^{-2} h^{-1}) after solvation with water, ethanol, acetone, hexane, toluene
8	Ref. 61 Chen et al. (Functionalized boron nitride membranes with ultrafast solvent transport performance for molecular separation) [61]	BN nanosheets deposited onto a porous nylon support	Dye rejection in organic solvents	90–100% rejection of congo red, methylene blue, evans blue in methanol for certain concentrations of the dye solutions
9	Ref. 57 Gonzalez-Ortiz et al. (Development of novel h-BNNS/PVA porous membranes: Via Pickering emulsion templating) [57]	BN nanosheets incorporated into a Polyvinyl alcohol matrix through pickering emulsion templating	Fouling resistance	76% rejection of polystyrene latex particles of 0.1 microns and 99.7% rejection of 1.2 micron size particles
10	Ref. 58 Low et al. (Fouling resistant 2D boron nitride nanosheet – PES nano filtration membranes) [58]	BN/PES mixed matrix membrane	Fouling resistance	Flux recovery ration of 100% after fouling with 1wt% humic acid
11	Ref. 59 Zahirifar et al. (Influence of hexagonal boron nitride nanosheets as the additives on the characteristics and performance of PVDF for air gap membrane distillation) [59]	BN/PVDF mixed matrix membrane	Enhanced thermal stability and permeance in membrane distillation	99% rejection of 3.5 wt% NaCl solution, along with a water flux of 7.1 kg m^{-2} h^{-1}

Table 1 (continued)

S. No	Reference	Architecture	Application	Performance
12	Ref. 41 Chen et al. (Ultrafast, Stable Ionic and Molecular Sieving through Functionalized Boron Nitride Membranes) [41]	BN nanosheets deposited onto a porous cellulose ester support	Enhance ion-permeation rates/ to compare permeation rates of various ions	Permeation rates of 1×10^{-3} mol h^{-1} m^{-2} for glycerol, sucrose and Mn^{2+} ions while permeation rates of 1–10 mol h^{-1} m^{-2} for Na^{+}, K^{+}, Ca^{2+}, Mg^{2+}, Zn^{2+}
13	Ref. 43 Pendse et al. (Charged Layered Boron Nitride-Nanoflake Membranes for Efficient Ion Separation and Water Purification) [43]	BN nanosheets deposited onto an anodized aluminium oxide porous support	Anion rejection	> 97% rejection for K_2SO_4, $MgSO_4$ as well as for anionic dyes such as congo red
14	Ref. 62 Lin et al. (Graphite oxide/boron nitride hybrid membranes: The role of cross-plane laminar bonding for a durable membrane with large water flux and high rejection rate) [62]	BN and GO nanosheets alternately deposited onapolydopamine coated porous PES support	Stabilization of GO, dye rejection	99.98% rejection of methylene blue, stable over 9 h
15	Ref. 63 Chen et al. (Bio-inspired Nanocomposite Membranes for Osmotic Energy Harvesting) [63]	BN/Aramid nanofiber composite membrane	Osmotic power generation	0.6 Wm^{-2} power density, retained over 200 h
16	Ref. 64 Yazda et al. (High Osmotic Power Generation via Nanopore Arrays in Hybrid Hexagonal Boron Nitride/Silicon Nitride Membranes) [64]	BN/SiN hybrid membrane	Osmotic power generation	Varied between 10–30 pW depending on the pore spacing
17	Ref. 66 Das et al. (High flux and adsorption based non-functionalized hexagonal boron nitride lamellar membrane for ultrafast water purification) [66]	BN nanosheets deposited onto a PVDF porous support	Dye rejection	> 90% rejection of methyl orange and direct red-80, adsorption capacitites for bisphenol A, methyl orange and direct red-80: 125.7, 120.8, and 328.2 mg/g
18	Ref. 65 Keshebo et al. (Simultaneous exfoliation and functionalization of hexagonal boron nitride in the aqueous phase for the synthesis of high-performance wastewater treatment membrane) [65]	BN nanosheets deposited onto a porous nylon support	Dye rejection, fouling resistance	90% rejection of methylene blue, rhodamine B and congo red, > 92% of initial flux maintained after 7 cycles
31	Ref. 67 Liang, G. et al. (Boron Nitride Ultrathin Fibrous Nanonets: One-Step Synthesis and Applications for Ultrafast Adsorption for Water Treatment and Selective Filtration of Nanoparticles) [67]	Nanonet made from BN nanofibres	Dye removal	327.8 mg/g of methylene blue adsorbed in 1 min
32	Ref. 68 Liang, G. et al. (Controlled Fabrication of Ultrathin-Shell BN Hollow Spheres with Excellent Performance in Hydrogen Storage and Wastewater Treatment) [68]	BN Nanospheres	Hydrogen storage, dye removal	Adsorption capacity for basic yellow 1 and methylene blue- 191.7 and 116.5 mg/g, hydrogen uptake capacity up to 4.07 wt.% at 298 K and 10 MPa
33	Ref. 69 Liu et al. (Nanosheet-Structured Boron Nitride Spheres with a Versatile Adsorption Capacity for Water Cleaning) [69]	BN spheres	Heavy metals and organic dye removal	Adsorption capacities for malachite green and methylene blue—324 and 233 mg/g, for Cu^{2+}, Pb^{2+}, and Cd^{2+} are 678.7, 536.7, and 107.0 mg/g

Table 1 (continued)

S. No	Reference	Architecture	Application	Performance
34	Ref. 44 Li J et al. (Activated Boron Nitride as an Effective Adsorbent for Metal Ions and Organic Pollutants) [44]	Porous BN ribbons	Heavy metal, antibiotic, dye removal	Adsorption capacity for Co^{2+}, Ni^{2+}, Ce^{3+}, and Pb^{2+}—215, 235, 282 and 225 mg/g, for tetracycline, methyl orange and congo red and 300–400 mg/g
35	Ref. 75 Li Jie et al. (Chemical Activation of Boron Nitride Fibers for Improved Cationic Dye Removal Performance) [75]	BN fibres	Dye removal	Adsorption capacity for methylene blue was 392.2 mg/g
36	Ref 76 Song et al. (The Performance of Porous Hexagonal BN in High Adsorption Capacity towards Antibiotics Pollutants from Aqueous Solution) [76]	Rod like porous BN	Antibiotic removal	adsorption capacity for tetracycline—322.16 mg/g
37	Ref 79 Jei Li et al. (NaOH-Embedded Three-Dimensional Porous Boron Nitride for Efficient Formaldehyde Removal) [79]	3D BN adsorbent	Formaldehyde adsorption	Adsorption capacity for formaldehyde > 350 mg/g
38	Ref 45 Yanming Xue et al. (Template-free synthesis of boron nitride foam-like porous monoliths and their high-end applications in water purification) [45]	Porous BN monolith	Heavy metal and dye removal	Adsorption capacity for rhodamine B and Cd^{2+} was 554 mg/g and 561 mg/g
39	Ref 80 Jun Yin et al. (Ultralight Three-Dimensional Boron Nitride Foam with Ultralow Permittivity and Superelasticity) [80]	BN foam	Proof of concept	-
40	Ref 84 Liu Z (Novel Multifunctional Cheese-like 3D Carbon-BN as a Highly Efficient Adsorbent for Water Purification) [84]	C-BN foam	Heavy metal and dye removal	Adsorption capacity for methylene blue and congo red was 402.25 mg/g and 307 mg/g, Cr^{3+} is 453.1 mg/g, Cd^{2+} and Ni^{2+} are 482.1 and 172.6 mg/g
41	Ref 86 Krishna Kumar et al. (Heavy Metal and Organic Dye Removal via a Hybrid Porous Hexagonal Boron Nitride-Based Magnetic Aerogel) [86]	BN nanosheets/Polyvinylalcohol foam	Heavy metal, dye removal	Adsorption capacity for Cr(VI), As(V), methylene blue, and acid orange was 833, 426, 415, 286 mg/g
42	Ref 87 Liu et al. (Layer-by-Layer Assembly Fabrication of Porous Boron Nitride Coated Multifunctional Materials for Water Cleaning) [87]	BN nanosheets deposited on cotton fabric or melamine	Oil–water separation	Adsorption ability for pump oil, white oil, and chloroform was in the range of 58–112 times its own weight

et al. prepared a 3D "cheese-like" C-BN with pore size ranging 2-100 nm, which could adsorb methylene blue and congo red, as well as Cr^{3+}, Cd^{2+}, Ni^{2+} from water. The group also demonstrated successful oil–water separation performance of C-BN with salad oil, gasoline, and pump oil. The adsorbent could be regenerated by heating at certain temperatures for a certain amount of time, and reused, as shown by the multiple regeneration-adsorption cycles (Fig. 7). The group combined the high adsorption capacity of boron nitride with that of carbon, with the C-BN hybrid material. Interesting point to note- the C-BN adsorbent was synthesized as a foam. But for dye and heavy metal removal tests it was ground into a powder, while for the oil–water separation tests the foam was used as is [84].

Composites of BN with polymers also offer excellent adsorption properties by exploiting the combined properties of BN as well as those of the polymer. Like in the case of mixed matrix membranes discussed in the previous section, dispersing various forms of BN in a polymer matrix to fabricate a foam, or directly depositing BN nanomaterials on already synthesized foams imparts structural stability to the entire architecture while enhancing the adsorption properties of the composite foams. For instance, Yu et al. fabricated a porous composite of BN nanosheets and PVDF for oil–water separation and demonstrated its application as a membrane as well as an adsorbent, exploiting the inherent hydrophobicity of BN and PVDF [85]. Krishna Kumar et al. fabricated polyethyleneimine modified hBN nanosheets, on which magnetite (Fe_3O_4) nanoparticles were grown, and were blended with polyvinyl alcohol and freeze dried to create an aerogel for heavy metal removal and organic dye removal. The magnetite nanoparticles enhanced the capacity for heavy metal adsorption [86]. Liu et al. coated BN nanosheets on cotton fabric and melamine sponge using a layer by layer assembly for enhanced oil–water separation and dye removal [87]. Similarly, Zhou et al. made BN deposited melamine foams for excellent oil–water separation and dye adsorption [88]. These studies demonstrate the application of BN as an adsorbent as is or by incorporating it into existing architectures, such as in the 3D porous structures, to exploit its properties that make it ideal for use as an adsorbent- low density, lightweight, high surface area to volume ratio, inherent hydrophobicity, ability to withstand high temperatures and harsh chemical environments without damaging its structural integrity, and high mechanical strength.

Table 1 reports the architectures and as well as the application of BN in water remediation in the references in this review, along with their corresponding performance.

Conclusions

The future of BN nanomaterials in water purification membranes looks promising. However, numerous challenges must be overcome to realize their full potential. The synthesis routes for fabricating most nanomaterials are complex, long-winded, and expensive, and often involve hazardous chemicals. For example, hydrogen fluoride is used to etch out Aluminium from the MAX phase of $Ti_3C_2T_x$ [28]. In the case of BN, its chemical inertness is a double-edged sword. On the one hand, it makes BN adsorbents easy to regenerate, prevents swelling and retains the sieving performance of laminar membranes in various solvents, but on the other hand renders the functionalization of BN quite difficult [40]. More effective, high-yielding methods of functionalization of BN are needed to alleviate these issues. When incorporated into a polymer matrix, aggregation of the nanomaterials presents a problem, which can be controlled by modifying the latter to aid matrix-filler interaction and dispersion. Laminar membranes formed by stacking these nanomaterials swell or disperse on hydration, which can affect the separation efficiency and durability. Unstable structures can also be leached out during filtration. Attaching additional functional groups, covalently cross-linking the sheets, and using the right porous support would solve these issues. Most filtration studies are conducted with a feed solution of one or few model micropollutants, which is far from the real feed water composition. Experiments, along with modelling and simulation studies must be carried out with complex feed matrices containing different types and levels of pollutants representative of the real compositions. This helps understand the selectivity of the 2D BN nanomaterials-based membrane for one pollutant in the presence of others.

Although laminar membranes of 2D nanomaterials show high water permeance, their desalination capacity has not yet reached that of polyamide membranes. Their selectivity depends on the electrostatic interaction and size-based exclusion. Engineering the surface charge and the nanochannels according to the desalination needs without compromising on the water permeance, would lead to the ideal desalination membranes. Transport mechanisms in 2D nanomaterials is an attractive field of study, as there is lot more yet to be understood, through modelling and simulation studies aided by carefully designed experiments [89].

Large scale, cost-effective manufacturing of defect-free BN nanomaterials with controlled dimensions, pore size and pore size distribution remains a challenge as quality of the material varies considerably across manufacturers [90]. The limited data on the environmental and health risks of engineered nanoparticles, although much less than perceived, can hinder plant

operators and regulators from adopting nanomaterials-based products in treatment plants. Therefore, more studies must be conducted on the environmental impacts of each of these engineered nanomaterials, especially in the presence of other pollutants [91]. From the review of the ongoing research efforts on BN nanomaterials, it can be concluded that BN nanomaterials possess remarkable potential in leading the new generation of water purification membranes and adsorbents, and it is worth investing our time and effort to overcome barriers to herald a new generation of architectures for efficient water purification.

Authors' contributions
SA wrote the main manuscript text and prepared the figures SB: Gave critical inputs and insights to various section of this review. All the authors reviewed the manuscript. The author(s) read and approved the final manuscript.

Funding
The authors would like to thank the Science and Engineering Research Board (SERB), Government of India for the financial support.

Availability of data and materials
Third party data has been used with permission, which will be provided upon request.

Declarations

Ethics approval and consent to particicpate
Not applicable.

Competing interests
The authors declare no competing interests.

Author details
[1]Department of Materials Engineering, Indian Institute of Science, Bengaluru 560012, India.

Received: 19 December 2022 Accepted: 6 April 2023
Published online: 24 April 2023

References

1. M. Stolov, V. Freger, Degradation of polyamide membranes exposed to chlorine: an impedance spectroscopy study. Environ. Sci. Technol. **53**(5), 2618–2625 (2019). https://doi.org/10.1021/acs.est.8b04790
2. D. Pakulski, W. Czepa, S.D. Buffa, A. Ciesielski, P. Samorì, Atom-thick membranes for water purification and blue energy harvesting. Adv. Funct. Mater. **30**(2), 1–21 (2020). https://doi.org/10.1002/adfm.201902394
3. J. Zhu, J. Hou, A. Uliana, Y. Zhang, M. Tian, B. Van Der Bruggen, The rapid emergence of two-dimensional nanomaterials for high-performance separation membranes. J. Mater. Chem. A **6**(9), 3773–3792 (2018). https://doi.org/10.1039/c7ta10814a
4. P.L. Jagadeshvaran, V. Menon, S. Bose, Evolution of personal protective equipment from its inception to COVID-19. Rev. Artic. Curr. Sci. **120**(7), 1169-1183 (2021)
5. S. Homaeigohar, M. Elbahri, Graphene membranes for water desalination. NPG Asia Mater. **9**(8), e427 (2017). https://doi.org/10.1038/am.2017.135
6. G. Wei, X. Quan, S. Chen, H. Yu, Superpermeable atomic-thin graphene membranes with high selectivity. ACS Nano **11**(2), 1920–1926 (2017). https://doi.org/10.1021/acsnano.6b08000
7. M.E. Suk, N.R. Aluru, Water transport through ultrathin graphene. J. Phys. Chem. Lett. **1**(10), 1590–1594 (2010). https://doi.org/10.1021/jz100240r
8. D. Cohen-Tanugi, J.C. Grossman, Water desalination across nanoporous graphene. Nano Lett. **12**(7), 3602–3608 (2012). https://doi.org/10.1021/nl3012853
9. S. Cerveny, F. Barroso-Bujans, Á. Alegría, J. Colmenero, Dynamics of water intercalated in graphite oxide. J. Phys. Chem. C **114**(6), 2604–2612 (2010). https://doi.org/10.1021/jp907979v
10. Y. Wei, Y. Zhang, X. Gao, Z. Ma, X. Wang, C. Gao, Multilayered graphene oxide membrane for water treatment: a review. Carbon **139**, 964–981 (2018). https://doi.org/10.1016/j.carbon.2018.07.040
11. T. Yang, H. Lin, K.P. Loh, B. Jia, Fundamental transport mechanisms and advancements of graphene oxide membranes for molecular separation. Chem. Mater. (2019). https://doi.org/10.1021/acs.chemmater.8b03820
12. W. Li, L. Zhang, X. Zhang, M. Zhang, T. Liu, S. Chen, Atomic insight into water and ion transport in 2D interlayer nanochannels of graphene oxide membranes: implication for desalination. J. Membr. Sci. **596**, 117744 (2020). https://doi.org/10.1016/j.memsci.2019.117744
13. S. Maiti, S. Bose, Free-standing graphene oxide membrane works in tandem with confined interfacial polymerization of polyamides towards excellent desalination and chlorine tolerance performance. Nanoscale Adv. **4**(2), 467–478 (2022). https://doi.org/10.1039/d1na00513h
14. N. Padmavathy, S.S. Behera, S. Pathan, L. Das Ghosh, S. Bose, Interlocked graphene oxide provides narrow channels for effective water desalination through forward osmosis. ACS Appl. Mater. Interfaces **11**(7), 7566–7575 (2019). https://doi.org/10.1021/acsami.8b20598
15. S. Zheng, Q. Tu, J.J. Urban, S. Li, B. Mi, Swelling of graphene oxide membranes in aqueous solution: characterization of interlayer spacing and insight into water transport mechanisms. ACS Nano **11**(6), 6440–6450 (2017). https://doi.org/10.1021/acsnano.7b02999
16. S. Remanan, N. Padmavathy, S. Ghosh, S. Mondal, S. Bose, N.C. Das, Porous graphene-based membranes: preparation and properties of a unique two-dimensional nanomaterial membrane for water purification. Sep. Purif. Rev. **50**(3), 262–282 (2021). https://doi.org/10.1080/15422119.2020.1725048
17. Q.H. Wang, K. Kalantar-Zadeh, A. Kis, J.N. Coleman, M.S. Strano, Electronics and optoelectronics of two-dimensional transition metal dichalcogenides. Nat. Publ. Group **7**, (2012). https://doi.org/10.1038/NNANO.2012.193
18. M. Heiranian, A.B. Farimani, N.R. Aluru, Water desalination with a single-layer MoS 2 nanopore. Nat. Commun. **6**, 1–6 (2015). https://doi.org/10.1038/ncomms9616
19. Z. Wang, Q. Tu, S. Zheng, J.J. Urban, S. Li, B. Mi, Understanding the aqueous stability and filtration capability of MoS2 membranes. Nano Lett. **17**(12), 7289–7298 (2017). https://doi.org/10.1021/acs.nanolett.7b02804
20. L. Sun, H. Huang, X. Peng, Laminar MoS2 membranes for molecule separation. Chem. Commun. **49**(91), 10718–10720 (2013). https://doi.org/10.1039/c3cc46136j
21. L. Ries, E. Petit, T. Michel, C.C. Diogo, C. Gervais, C. Salameh, M. Bechelany, S. Balme, P. Miele, N. Onofrio, D. Voiry, Enhanced sieving from exfoliated MoS2 membranes via covalent functionalization. Nat. Mater. **18**(10), 1112–1117 (2019). https://doi.org/10.1038/s41563-019-0464-7
22. F. Zhao, M. Peydayesh, Y. Ying, J. Ping, in *Transition Metal Dichalcogenide — Silk Nano Fi Bril Membrane for One- Step Water Puri Fi Cation and Precious Metal Recovery* (2020). https://doi.org/10.1021/acsami.0c07846
23. J. Ma, X. Tang, Y. He, Y. Fan, J. Chen, HaoYu, Robust stable MoS2/GO filtration membrane for effective removal of dyes and salts from water with enhanced permeability. Desalination **480**(December 2019), 114328 (2020). https://doi.org/10.1016/j.desal.2020.114328
24. C.L. Fausey, I. Zucker, D.E. Lee, E. Shaulsky, J.B. Zimmerman, M. Elimelech, Tunable molybdenum disulfide-enabled fiber mats for high-efficiency removal of mercury from water. ACS Appl. Mater. Interfaces **12**(16), 18446–18456 (2020). https://doi.org/10.1021/acsami.9b22823
25. F. Jia, Q. Wang, J. Wu, Y. Li, S. Song, Two-dimensional molybdenum disulfide as a superb adsorbent for removing Hg2+ from water. ACS Sustain. Chem. Eng. **5**(8), 7410–7419 (2017). https://doi.org/10.1021/acssuschemeng.7b01880
26. P.K. Samantaray, S. Baloda, G. Madras, S. Bose, Interlocked dithi-magnetospheres–decorated MoS 2 nanosheets as molecular sieves and traps for heavy metal ions. Adv. Sustain. Syst. **3**(6), 1800153 (2019). https://doi.org/10.1002/adsu.201800153

27. M. Naguib, V.N. Mochalin, M.W. Barsoum, Y. Gogotsi, 25th anniversary article: MXenes: a new family of two-dimensional materials. Adv. Mater. **26**(7), 992–1005 (2014). https://doi.org/10.1002/adma.201304138
28. I. Ihsanullah, MXenes (two-dimensional metal carbides) as emerging nanomaterials for water purification: progress, challenges and prospects. Chem. Eng. J. **2020**(388), 124340 (2019). https://doi.org/10.1016/j.cej.2020.124340
29. M. Naguib, M. Kurtoglu, V. Presser, J. Lu, J. Niu, M. Heon, L. Hultman, Y. Gogotsi, M.W. Barsoum, Two-dimensional nanocrystals produced by exfoliation of Ti 3AlC 2. Adv. Mater. **23**(37), 4248–4253 (2011). https://doi.org/10.1002/adma.201102306
30. C.E. Ren, K.B. Hatzell, M. Alhabeb, Z. Ling, K.A. Mahmoud, Y. Gogotsi, Charge- and size-selective ion sieving through Ti3C2Tx MXene membranes. J. Phys. Chem. Lett. **6**(20), 4026–4031 (2015). https://doi.org/10.1021/acs.jpclett.5b01895
31. K. Rasool, M. Helal, A. Ali, C.E. Ren, Y. Gogotsi, K.A. Mahmoud, Antibacterial activity of Ti3C2Tx MXene. ACS Nano **10**(3), 3674–3684 (2016). https://doi.org/10.1021/acsnano.6b00181
32. K. Rasool, K.A. Mahmoud, D.J. Johnson, M. Helal, G.R. Berdiyorov, Y. Gogotsi, Efficient antibacterial membrane based on two-dimensional Ti3C2Tx (MXene) nanosheets. Sci. Rep. **7**(1), 1598 (2017). https://doi.org/10.1038/s41598-017-01714-3
33. O.-S. Lee, M.E. Madjet, K.A. Mahmoud, Antibacterial mechanism of multifunctional MXene nanosheets: domain formation and phase transition in lipid bilayer. Nano Lett. **21**(19), 8510–8517 (2021). https://doi.org/10.1021/acs.nanolett.1c01986
34 K. Salimiyan Rizi, MXene nanosheets as a novel nanomaterial with antimicrobial applications: a literature review. J. Mol. Struct. **1262**, 132958 (2022). https://doi.org/10.1016/j.molstruc.2022.132958
35. J. Saththasivam, K. Wang, W. Yiming, Z. Liu, K.A. Mahmoud, A flexible Ti3C2Tx (MXene)/paper membrane for efficient oil/water separation. RSC Adv. **9**(29), 16296–16304 (2019). https://doi.org/10.1039/c9ra02129a
36. X.-J. Zha, X. Zhao, J.-H. Pu, L.-S. Tang, K. Ke, R.-Y. Bao, L. Bai, Z.-Y. Liu, M.-B. Yang, W. Yang, Flexible anti-biofouling MXene/cellulose fibrous membrane for sustainable solar-driven water purification. ACS Appl. Mater. Interfaces (2019). https://doi.org/10.1021/acsami.9b10606
37. L. Ding, Y. Wei, Y. Wang, H. Chen, J. Caro, H. Wang, A two-dimensional lamellar membrane: MXene nanosheet stacks. Angew. Chem. - Int. Ed. **56**(7), 1825–1829 (2017). https://doi.org/10.1002/anie.201609306
38. X. Wang, Functionalized hexagonal boron nitride nanomaterials : emerging properties and applications include the controlled synthesis. Chem. Soc. Rev. **45**, 3989–4012 (2016). https://doi.org/10.1039/c5cs00869g
39 K. Zhang, Y. Feng, F. Wang, Z. Yang, J. Wang, Two dimensional hexagonal boron nitride (2D-HBN): synthesis, properties and applications. J. Mater. Chem. C **5**(46), 11992–12022 (2017). https://doi.org/10.1039/c7tc04300g
40. W. Lei, V.N. Mochalin, D. Liu, S. Qin, Y. Gogotsi, Y. Chen, Boron nitride colloidal solutions, ultralight aerogels and freestanding membranes through one-step exfoliation and functionalization. Nat. Commun. **6**, 1–8 (2015). https://doi.org/10.1038/ncomms9849
41. C. Chen, S. Qin, D. Liu, J. Wang, G. Yang, Y. Su, L. Zhang, W. Cao, M. Ma, Y. Qian, Y. Liu, J.Z. Liu, W. Lei, Ultrafast, stable ionic and molecular sieving through functionalized boron nitride membranes. ACS Appl. Mater. Interfaces (2019). https://doi.org/10.1021/acsami.9b08296
42. S. Abdikheibari, W. Lei, L.F. Dumée, N. Milne, K. Baskaran, Thin film nanocomposite nanofiltration membranes from amine functionalized-boron nitride/polypiperazine amide with enhanced flux and fouling resistance. J. Mater. Chem. A **6**(25), 12066–12081 (2018). https://doi.org/10.1039/C8TA03446J
43. A. Pendse, S. Cetindag, M.H. Lin, A. Rackovic, R. Debbarma, S. Almassi, B.P. Chaplin, V. Berry, J.W. Shan, S. Kim, Charged layered boron nitride-nanoflake membranes for efficient ion separation and water purification. Small **15**(49), e1904590 (2019). https://doi.org/10.1002/smll.201904590
44. J. Li, X. Xiao, X. Xu, J. Lin, Y. Huang, Y. Xue, P. Jin, J. Zou, C. Tang, Activated boron nitride as an effective adsorbent for metal ions and organic pollutants. Sci. Rep. **3**, 1–7 (2013). https://doi.org/10.1038/srep03208
45. Y. Xue, P. Dai, X. Jiang, X. Wang, C. Zhang, D. Tang, Q. Weng, X. Wang, A. Pakdel, C. Tang, Y. Bando, D. Golberg, Template-free synthesis of boron nitride foam-like porous monoliths and their high-end applications in water purification. J. Mater. Chem. A **4**(4), 1469–1478 (2015). https://doi.org/10.1039/c5ta08134c
46. M. Li, G. Huang, X. Chen, J. Yin, P. Zhang, Y. Yao, J. Shen, Y. Wu, J. Huang, Perspectives on environmental applications of hexagonal boron nitride nanomaterials. Nano Today **44**, 101486 (2022). https://doi.org/10.1016/j.nantod.2022.101486
47. J. Xiong, J. Di, W. Zhu, H. Li, Hexagonal boron nitride adsorbent: synthesis, performance tailoring and applications. J. Energy Chem. **40**, 99–111 (2020). https://doi.org/10.1016/j.jechem.2019.03.002
48. Ö. Şen, M. Emanet, M. Çulha, Stimulatory effect of hexagonal boron nitrides in wound healing. ACS Appl. Bio Mater. **2**(12), 5582–5596 (2019). https://doi.org/10.1021/acsabm.9b00669
49. H. Ghorbanfekr, J. Behler, F.M. Peeters, Insights into water permeation through HBN nanocapillaries by Ab Initio machine learning molecular dynamics simulations. J. Phys. Chem. Lett. **11**(17), 7363–7370 (2020). https://doi.org/10.1021/ACS.JPCLETT.0C01739/SUPPL_FILE/JZ0C01739_SI_001.PDF
50. G. Tocci, L. Joly, A. Michaelides, Friction of water on graphene and hexagonal boron nitride from Ab Initio methods: very different slippage despite very similar interface structures. Nano Lett. **14**(12), 6872–6877 (2014). https://doi.org/10.1021/nl502837d
51. L. Liu, Y. Liu, Y. Qi, M. Song, L. Jiang, G. Fu, J. Li, Hexagonal boron nitride with nanoslits as a membrane for water desalination: a molecular dynamics investigation. Sep. Purif. Technol. **251**, 117409 (2020). https://doi.org/10.1016/J.SEPPUR.2020.117409
52. R. Jafarzadeh, J. Azamat, H. Erfan-Niya, M. Hosseini, Molecular insights into effective water desalination through functionalized nanoporous boron nitride nanosheet membranes. Appl. Surf. Sci. **471**, 921–928 (2019). https://doi.org/10.1016/j.apsusc.2018.12.069
53. W. Lei, D. Portehault, D. Liu, S. Qin, Y. Chen, Porous boron nitride nanosheets for effective water cleaning. Nat. Commun. **4**, 1–7 (2013). https://doi.org/10.1038/ncomms2818
54. D. Liu, L. He, W. Lei, K.D. Klika, L. Kong, Y. Chen, Multifunctional polymer/porous boron nitride nanosheet membranes for superior trapping emulsified oils and organic molecules. Adv. Mater. Interfaces **2**(12), 1–6 (2015). https://doi.org/10.1002/admi.201500228
55. C. Marichy, V. Salles, X. Jaurand, A. Etiemble, T. Douillard, J. Faugier-Tovar, F. Cauwet, A. Brioude, Fabrication of BN membranes containing high density of cylindrical pores using an elegant approach. RSC Adv. **7**(34), 20709–20715 (2017). https://doi.org/10.1039/C7RA03808A
56. S. Abdikheibari, W. Lei, L.F. Dumée, A.J. Barlow, K. Baskaran, Novel thin film nanocomposite membranes decorated with few-layered boron nitride nanosheets for simultaneously enhanced water flux and organic fouling resistance. Appl. Surf. Sci. **488**(April), 565–577 (2019). https://doi.org/10.1016/j.apsusc.2019.05.217
57. D. Gonzalez-Ortiz, C. Pochat-Bohatier, S. Gassara, J. Cambedouzou, M. Bechelany, P. Miele, Development of novel H-BNNS/PVA porous membranes: via pickering emulsion templating. Green Chem. **20**(18), 4319–4329 (2018). https://doi.org/10.1039/c8gc01983e
58. Z. Low, J. Ji, D. Blumenstock, Y. Chew, D. Wolverson, D. Mattia, Fouling resistant 2D boron nitride nanosheet – PES nanofiltration membranes. J. Membr. Sci. **563**(April), 949–956 (2018). https://doi.org/10.1016/j.memsci.2018.07.003
59. J. Zahirifar, A. Hadi, J. Karimi-Sabet, A. Dastbaz, Influence of hexagonal boron nitride nanosheets as the additives on the characteristics and performance of PVDF for air gap membrane distillation. Desalination **460**(April 2018), 81–91 (2019). https://doi.org/10.1016/j.desal.2019.03.004
60. C. Chen, D. Liu, J. Wang, L. Wang, J. Sun, W. Lei, Functionalized boron nitride membranes with multipurpose and super-stable semi-permeability in solvents. J. Mater. Chem. A **6**(42), 21104–21109 (2018). https://doi.org/10.1039/C8TA06161K
61 C. Chen, J. Wang, D. Liu, C. Yang, Y. Liu, R.S. Ruoff, W. Lei, Functionalized boron nitride membranes with ultrafast solvent transport performance for molecular separation. Nat. Commun. **9**(1), 1902 (2018). https://doi.org/10.1038/s41467-018-04294-6
62. H. Lin, N. Mehra, Y. Li, J. Zhu, Graphite oxide/boron nitride hybrid membranes: the role of cross-plane laminar bonding for a durable membrane with large water flux and high rejection rate. J. Membr. Sci. **593**(August 2019), 117401 (2020). https://doi.org/10.1016/j.memsci.2019.117401
63. C. Chen, D. Liu, L. He, S. Qin, J. Wang, J.M. Razal, N.A. Kotov, W. Lei, Bio-inspired nanocomposite membranes for osmotic energy harvesting. Joule **4**(1), 247–261 (2020). https://doi.org/10.1016/j.joule.2019.11.010

64. K. Yazda, K. Bleau, Y. Zhang, X. Capaldi, T. St-Denis, P. Grutter, W.W. Reisner, High osmotic power generation via nanopore arrays in hybrid hexagonal boron nitride/silicon nitride membranes. Nano Lett. **21**, 4152–4159 (2021). https://doi.org/10.1021/ACS.NANOLETT.0C04704
65. D.L. Keshebo, C.-C. Hu, W.-S. Hung, C.-F. Wang, H.-C. Tsai, K.-R. Lee, J.-Y. Lai, Simultaneous exfoliation and functionalization of hexagonal boron nitride in the aqueous phase for the synthesis of high-performance wastewater treatment membrane. J. Clean. Prod. **314**, 128083 (2021). https://doi.org/10.1016/J.JCLEPRO.2021.128083
66. R. Das, P. Solís-Fernández, D. Breite, A. Prager, A. Lotnyk, A. Schulze, H. Ago, High flux and adsorption based non-functionalized hexagonal boron nitride lamellar membrane for ultrafast water purification. Chem. Eng. J. **420**, 127721 (2021). https://doi.org/10.1016/J.CEJ.2020.127721
67. G. Lian, X. Zhang, H. Si, J. Wang, D. Cui, Q. Wang, Boron nitride ultrathin fibrous nanonets: one-step synthesis and applications for ultrafast adsorption for water treatment and selective filtration of nanoparticles. ACS Appl. Mater. Interfaces **5**(24), 12773–12778 (2013). https://doi.org/10.1021/am403789c
68. G. Lian, X. Zhang, S. Zhang, D. Liu, D. Cui, Q. Wang, Controlled fabrication of ultrathin-shell BN hollow spheres with excellent performance in hydrogen storage and wastewater treatment. Energy Environ. Sci. **5**(5), 7072 (2012). https://doi.org/10.1039/c2ee03240f
69. F. Liu, J. Yu, X. Ji, M. Qian, Nanosheet-structured boron nitride spheres with a versatile adsorption capacity for water cleaning. ACS Appl. Mater. Interfaces **7**(3), 1824–1832 (2015). https://doi.org/10.1021/am507491z
70. A. Nag, K. Raidongia, K.P.S.S. Hembram, R. Datta, U.V. Waghmare, C.N.R. Rao, Graphene analogues of BN: novel synthesis and properties. ACS Nano **4**(3), 1539–1544 (2010). https://doi.org/10.1021/nn9018762
71. Z. Zhou, J. Zhao, Z. Chen, X. Gao, T. Yan, B. Wen, P.V.R. Schleyer, Comparative study of hydrogen adsorption on carbon and BN nanotubes. J. Phys. Chem. B **110**(27), 13363–13369 (2006). https://doi.org/10.1021/jp0622740
72. J.F. Janik, W.C. Ackerman, R.T. Paine, D.-W. Hua, A. Maskara, D.M. Smith, Boron nitride as a selective gas adsorbent. Langmuir **10**(2), 514–518 (1994). https://doi.org/10.1021/la00014a029
73. Q. Sun, Z. Li, D.J. Searles, Y. Chen, G. Lu, A. Du, Charge-controlled switchable CO2 capture on boron nitride nanomaterials. J. Am. Chem. Soc. **135**(22), 8246–8253 (2013). https://doi.org/10.1021/ja400243r
74. J. Liang, Q. Song, J. Lin, G. Li, Y. Fang, Z. Guo, Y. Huang, C.-S. Lee, C. Tang, In situ Cu-loaded porous boron nitride nanofiber as an efficient adsorbent for CO_2 capture. ACS Sustain. Chem. Eng. **8**(19), 7454–7462 (2020). https://doi.org/10.1021/acssuschemeng.0c01530
75. J. Li, Y. Huang, Z. Liu, J. Zhang, X. Liu, H. Luo, Y. Ma, X. Xu, Y. Lu, J. Lin, J. Zou, C. Tang, Chemical activation of boron nitride fibers for improved cationic dye removal performance. J. Mater. Chem. A **3**(15), 8185–8193 (2015). https://doi.org/10.1039/C5TA00601E
76. Q. Song, Y. Fang, Z. Liu, L. Li, Y. Wang, J. Liang, Y. Huang, J. Lin, L. Hu, J. Zhang, C. Tang, The performance of porous hexagonal BN in high adsorption capacity towards antibiotics pollutants from aqueous solution. Chem. Eng. J. **325**, 71–79 (2017). https://doi.org/10.1016/j.cej.2017.05.057
77. Y. Chao, W. Zhu, J. Chen, P. Wu, X. Wu, H. Li, C. Han, S. Yan, Development of novel graphene-like layered hexagonal boron nitride for adsorptive removal of antibiotic gatifloxacin from aqueous solution. Green Chem. Lett. Rev. **7**(4), 330–336 (2014). https://doi.org/10.1080/17518253.2014.944941
78. Z. Li, X. Zhao, X. Hong, H. Yang, D. Fang, Y. Wang, M. Lei, Hierarchically porous boron nitride nanoribbon for safe and high-performance bisphenol A adsorption. Mater. Lett. **307**, 131022 (2022). https://doi.org/10.1016/j.matlet.2021.131022
79. J. Li, H. Jia, Y. Ding, H. Luo, S. Abbas, Z. Liu, L. Hu, C. Tang, NaOH-embedded three-dimensional porous boron nitride for efficient formaldehyde removal. Nanotechnology **26**(47), 475704 (2015). https://doi.org/10.1088/0957-4484/26/47/475704
80. J. Yin, X. Li, J. Zhou, W. Guo, Ultralight three-dimensional boron nitride foam with ultralow permittivity and superelasticity. Nano Lett. **13**(7), 3232–3236 (2013). https://doi.org/10.1021/nl401308v
81. C. Li, G. Shi, Three-Dimensional Graphene Architectures. Nanoscale **4**(18), 5549 (2012). https://doi.org/10.1039/c2nr31467c
82. H. Bi, X. Xie, K. Yin, Y. Zhou, S. Wan, L. He, F. Xu, F. Banhart, L. Sun, R.S. Ruoff, Spongy graphene as a highly efficient and recyclable sorbent for oils and organic solvents. Adv. Funct. Mater. **22**(21), 4421–4425 (2012). https://doi.org/10.1002/adfm.201200888
83. X. Zhang, G. Lian, S. Zhang, D. Cui, Q. Wang, Boron nitride nanocarpets: controllable synthesis and their adsorption performance to organic pollutants. CrystEngComm **14**(14), 4670 (2012). https://doi.org/10.1039/c2ce06748j
84. Z. Liu, Y. Fang, H. Jia, C. Wang, Q. Song, L. Li, J. Lin, Y. Huang, C. Yu, C. Tang, Novel multifunctional cheese-like 3D carbon-BN as a highly efficient adsorbent for water purification. Sci. Rep. **8**(1), 1104 (2018). https://doi.org/10.1038/s41598-018-19541-5
85. Y. Yu, H. Chen, Y. Liu, V.S.J. Craig, C. Wang, L.H. Li, Y. Chen, Superhydrophobic and superoleophilic porous boron nitride nanosheet/polyvinylidene fluoride composite material for oil-polluted water cleanup. Adv. Mater. Interfaces **2**(1), 1400267 (2015). https://doi.org/10.1002/admi.201400267
86. A.S. Krishna Kumar, J. Warchol, J. Matusik, W.-L. Tseng, N. Rajesh, T. Bajda, Heavy metal and organic dye removal via a hybrid porous hexagonal boron nitride-based magnetic aerogel. NPJ Clean Water **5**(1), 24 (2022). https://doi.org/10.1038/s41545-022-00175-0
87. D. Liu, M. Zhang, L. He, Y. Chen, W. Lei, Layer-by-layer assembly fabrication of porous boron nitride coated multifunctional materials for water cleaning. Adv. Mater. Interfaces **4**(16), 1700392 (2017). https://doi.org/10.1002/admi.201700392
88. Y. Zhou, Y. Wang, T. Liu, G. Xu, G. Chen, H. Li, L. Liu, Q. Zhuo, J. Zhang, C. Yan, Superhydrophobic HBN-regulated sponges with excellent absorbency fabricated using a green and facile method. Sci. Rep. **7**(1), 45065 (2017). https://doi.org/10.1038/srep45065
89. L. Wang, M.S.H. Boutilier, P.R. Kidambi, D. Jang, N.G. Hadjiconstantinou, R. Karnik, Fundamental transport mechanisms, fabrication and potential applications of nanoporous atomically thin membranes. Nat. Nanotechnol. **12**(6), 509–522 (2017). https://doi.org/10.1038/nnano.2017.72
90. L. Prozorovska, P.R. Kidambi, State-of-the-art and future prospects for atomically thin membranes from 2D materials. Adv. Mater. (2018). https://doi.org/10.1002/adma.201801179
91. P. Westerhoff, A. Atkinson, J. Fortner, M.S. Wong, J. Zimmerman, J. Gardea-Torresdey, J. Ranville, P. Herckes, Low risk posed by engineered and incidental nanoparticles in drinking water. Nat. Nanotechnol. **13**(8), 661–669 (2018). https://doi.org/10.1038/s41565-018-0217-9

Publisher's Note